Applied Energy 348 (2023) 121429

Contents lists available at ScienceDirect

Applied Energy

journal homepage: www.elsevier.com/locate/apenergy

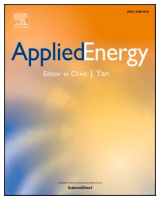

Resilience-oriented operation of microgrids in the presence of power-to-hydrogen systems

Vahid Shahbazbegian [a,*], Miadreza Shafie-khah [a], Hannu Laaksonen [a], Goran Strbac [b], Hossein Ameli [b,*]

[a] School of Technology and Innovations, University of Vaasa, Vaasa, Finland
[b] Control and Power Group, Imperial College London, London, UK

HIGHLIGHTS

- A model to operate PtH in microgrids considering industry demand for hydrogen.
- A novel approach to improve resiliency of microgrids in islanded mode.
- A bi-objective operation cost and resilience measures optimization model (MINLP).
- A solving approach based on the integration of GBD and MOGP methods.

ARTICLE INFO

Keywords:
Decomposition approach
Goal programming
Microgrid
Optimal operation
Power-to-hydrogen systems
Resilience

ABSTRACT

This study presents a novel framework for improving the resilience of microgrids based on the power-to-hydrogen concept and the ability of microgrids to operate independently (i.e., islanded mode). For this purpose, a model is being developed for the resilient operation of microgrids in which the compressed hydrogen produced by power-to-hydrogen systems can either be used to generate electricity through fuel cells or sold to other industries. The model is a bi-objective optimization problem, which minimizes the cost of operation and resilience by (i) reducing the active power exchange with the main grid, (ii) reducing the ohmic power losses, and (iii) increasing the amount of hydrogen stored in the tanks. A solution approach is also developed to deal with the complexity of the bi-objective model, combining a goal programming approach and Generalized Benders Decomposition, due to the mixed-integer nonlinear nature of the optimization problem. The results indicate that the resilience approach, although increasing the operation cost, does not lead to load shedding in the event of main grid failures. The study concludes that integrating distributed power-to-hydrogen systems results in significant benefits, including emission reductions of up to 20 % and cost savings of up to 30 %. Additionally, the integration of the decomposition method improves computational performance by 54 % compared to using commercial solvers within the GAMS software.

1. Introduction

1.1. Motivations and aims

The deployment of renewable energy resources is an option to mitigate the emissions of greenhouse gases which have become one of the major concerns on a global scale. Taking advantage of renewable resources, the federal government of the United States has set a goal of reaching a net-zero electricity sector by 2050 [1]. Likewise, the European Union plans to become climate-neutral by 2035, which will require the utilization of renewable resources, as energy production accounts for a substantial portion of global greenhouse gas emissions [2]. In order to ensure a reliable electricity supply using renewable resources, deploying distributed energy resources, such as rooftop photovoltaic panels and small-scale wind turbines, are potential options [3]. These units are installed in low-voltage electricity distribution networks near the consumers, which reduces transmission loss. It also increases the reliability of supply compared to traditional generators that are typically located far from consumers and mounted on high-

* Corresponding authors.
E-mail addresses: vahid.shahbazbegian@uwasa.fi (V. Shahbazbegian), miadreza.shafiekhah@uwasa.fi (M. Shafie-khah), hannu.laaksonen@uwasa.fi (H. Laaksonen), g.strbac@imperial.ac.uk (G. Strbac), h.ameli14@imperial.ac.uk (H. Ameli).

https://doi.org/10.1016/j.apenergy.2023.121429
Received 19 March 2023; Received in revised form 23 May 2023; Accepted 9 June 2023
Available online 13 July 2023

Nomenclature

Sets

I	Nodes in microgrid ($i \in I$)
T	Periods ($t \in T$)
L	Electric lines ($l \in L \subseteq (i, i')$)
C	Power-to-hydrogen systems consist of electrolyzers, hydrogen storage systems, and fuel cells ($c \in C \subseteq I$)

Parameters

$\delta_{i,t}$	Purchased energy price ($/kW)
$\delta'_{i,t}$	Sold energy price ($/kW)
δ'_{c}	Sold hydrogen price ($/m^3)
α_i	Variable cost of generating power using non-renewable dispatchable units ($/kW)
β_i	Cost of emissions ($/Ton)
ζ_i	Produced emissions of dispatchable units (Ton/kW)
γ_i	Fixed cost of generating power using non-renewable dispatchable units ($)
υ_i	Cost of load shedding ($/kW)
$P_i^{min/max}$	Minimum/maximum produced power by non-renewable units or supplied by substations (kW/h)
$R_i^{max\ up/down}$	Maximum ramp up/down of non-renewable units (kW/h)
$Q_i^{min/max}$	Minimum/maximum active power of non-renewable units or substations (kVAr)
$P_{i,t}^{load}$	Active demand (kW)
$Q_{i,t}^{load}$	Reactive demand (KVAr)
R_l	Resistance (Ω)
X_l	Reactance (Ω)
Z_l	Impedance (Ω)
$V_i^{min/max}$	Minimum/maximum voltage (kV)
I_l^{max}	Maximum current (kA)
$P_{i,t}^{wind,\ max}$	Maximum available power by wind generators (kW)
$\lambda, \mathscr{L}, \mathscr{L}', \wp, \mathscr{M}$	Optimal multipliers of optimization problem
ϕ_c	Efficiency of power-to-hydrogen (%)
φ_c	Efficiency of hydrogen-to-power (%)
ψ_c	Coefficient of hydrogen-to-power (kW/m^3)
$HL_{c,t}^{max}$	Maximum level of hydrogen through hydrogen storage systems (m^3)
HL_c^0	Initial level of hydrogen through hydrogen storage systems (m^3)
PN	Penalty

Decision variables

Z	Objective function
$\mathscr{R}$	Resiliency measures
$P_{i,t}^{buy/sell}$	Purchased/sold energy from/to day-ahead market (kW)
$P_{i,t}$	Generated power of non-renewable units (kW)
$Q_{i,t}$	Reactive power of generating units or substations (kVAr)
$P_{i,t}^{wind}$	Output power of wind turbines (kW)
$P_{i,t}^{line}$	Active power (kW)
$Q_{i,t}^{line}$	Reactive power (kVAr)
$I_{l,t}$	Electricity current (kA)
$V_{i,t}$	Voltage magnitude (kV)
$P_{c,t}^{E\rightarrow H_2}$	Electricity power used to produce hydrogen (kW)
$P_{c,t}^{H_2\rightarrow E}$	Produced power using hydrogen (kW)
$H_{c,t}^{in/out}$	Input/output volume of hydrogen (m^3)
$HL_{c,t}$	Volume of hydrogen through hydrogen storage systems (m^3)
$H_{c,t}^{E}$	Volume of hydrogen used to produce electricity (m^3)
$H_{c,t}^{sell}$	Volume of hydrogen sold to industries (m^3)
$P_{j,t}^{lsh}$	Load shedding (kW)
$SV_{i,t}^{s/d}$	Slack variables on supply/demand side

Binary variables

$u_{i,t}$	Status of non-renewable dispatchable units {1,0}
$\rho_{c,t}$	Injecting output power of fuel cells into microgrid using compressed hydrogen {1,0}
$\varrho_{c,t}$	Selling hydrogen to industries {1,0}

voltage transmission networks.

In order to operate distributed energy resources more efficiently, the sources and loads can be considered in an interconnected energy system called a "microgrid". Despite being generally connected to the main grid, the microgrid can operate autonomously, called islanded mode, when the upstream grid fails [4]. In this way, microgrids can improve the resilience of the electricity system by reducing the amount of energy-not-supplied. The term resiliency refers to the systems' ability to resist low-frequency and high-impact incidents efficiently and provide quick recovery and restoration [5]. Besides, excess microgrid generation can be sold to the main grid to provide customers with financial benefits, such as reductions in electricity bills. These factors make microgrids increasingly attractive to customers who cannot rely on the main grid and/or seek economic benefits from locally generated electricity. In the United States, microgrids operate in different states, and according to the forecasts, the capacity is expected to double to a total of 320 in the next three years [6]. There are also over 160 microgrids in India that mainly rely on solar panels for their power supply [7]. In addition to developed countries, microgrids can be an effective solution to connect people in developing and underdeveloped countries to electricity.

In addition to distributed energy resources, other options can come together in a microgrid, such as flexible small-scale generating units and power-to-hydrogen (PtH) systems. The flexible and dispatchable generating units are an appropriate option to handle the variability of renewable energy resources benefiting from their flexible ramping capability [8]. Moreover, PtH systems are flexible technologies that can convert the excess output of renewable energy resources and/or excess supply in electricity networks to hydrogen. This gas can be either consumed in other industries or converted to electricity to provide supply–demand balance during peak hours (e.g., using fuel cells) [9].

Despite the already-mentioned issues, solving the optimal operation of microgrids for the dispatch of different components is still challenging. The first reason would be the complexity of modeling different components, such as distributed generators, PtH systems, and storage systems. The second one would be difficulty with modeling power flow within the electricity network in microgrids, which involves a set of nonlinear constraints. Therefore, it would be more efficient to break the original problem into smaller ones and solve the subproblems, which decreases complexity compared to solving the original problem [10]. However, a solving procedure that finds optimal solutions to the problem should not sacrifice optimally and accuracy [11].

1.2. Review of related literature

A few review papers published recently investigating the operation of microgrids when distributed sources of renewable energy and Power-to-Gas (PtG) systems are highly prevalent. For instance, in [12], the role of different technologies and shares of PtG systems integrated into

energy systems are investigated and compared. In particular, different types of electrolyzers and storage systems were examined, along with a high and low penetration of the PtG systems. In [13], distinct aspects of energy systems, including PtG systems integration, resiliency consideration, pollution reduction, and operation objectives, are investigated. In [14], the operation of different storage systems, such as hydrogen storage systems, is recapped in energy systems. In the following, a systematic review of the recent research works in this field is also conducted as well. In this section, the studies in this field are divided based on their objectives, including examination of the role of PtG systems, resiliency consideration, or development of solving methods (e.g., heuristic and exact methods).

Among the previous studies, in [15], the role of PtG systems was studied costal microgrids in coastal areas considering water resources and wind power as energy input and raw material input, respectively. It concluded that the integration of PtG systems was an efficient solution to handle fluctuations of wind power by peak shaving and valley filling. In [16], a considerable number of PtG systems were examined in islanded microgrids applying a game that involves different parties, including wind turbines, storage systems, and photovoltaic systems. The results indicated the integration of hydrogen and methane reduced wind curtailment and improved the income of each party. In [17], the effect of PtG systems and fuel cells was examined in the optimal operation and planning of microgrids. It was demonstrated that the integration of the PtG systems improved the penetration level of renewable resources to supply demand. In [18], the role of PtG systems besides fuel-cell electric vehicles was investigated to mitigate the growth in energy demand due to the development of the transportation system. It indicated that the integration of PtG systems assisted in the integration of electric vehicles by decreasing renewable energy curtailment. In [19], the study focused on assessing the effects of PtG and power-to-heat technologies on the operation of industrial microgrids, with the aim of providing affordable energy supply to meet the demand. The operator of the industrial parks interacted with different markets (e.g., the heat market), which provided operating cost savings. Some studies also examined the effect of PtG systems in conjunction with the combined heat and power systems. For instance, in [20] and [21], the role of PtG systems and combined cooling and heating systems were examined to enhance clean production in microgrids. In [22] and [23], the joint dispatch of PtG systems and combined heat and power systems were considered to handle the variability of renewable energy resources and demand. These studies also demonstrated that integrating PtG systems into microgrids reduced operating costs and emissions. In [24] and [25], the problem of optimal operation of microgrids was examined by considering PtG systems, combined heat and power systems, and fuel cell electric vehicles. The obtained results indicated that the combination of the technologies and electric vehicles reduced the operating costs of microgrids. In [26] and [27], the effect of PtG systems and demand response programs on scheduling microgrids was studied by considering combined heat and power units. In [28], the impacts of PtG systems and demand response programs were studied on scheduling microgrids coupled with wind turbines, photovoltaic systems, and storage systems. These studies showed that the integration of PtG systems into demand response programs or storage systems was an appropriate solution to reach peak shaving and valley filling that leads to operating cost savings. Besides, some other studies consider other subsystems' constraints in operating microgrids to examine the impact of PtG systems (e.g., gas, hydrogen, and heat networks). In [29], the role of PtG facilities was examined by considering a hydrogen subsystem to be utilized for the charging station of electric vehicles in microgrids. In [30], the impact of PtG systems was studied on microgrids considering congestion in the natural gas network. The results of the studies indicated that the output hydrogen of PtG systems supplied electric vehicles and injected into the gas network, respectively, which concluded cost savings. In [31], the variation of market price and wind power, as well as the role of hydrogen storage systems in microgrids, were studied, which consisted of the electricity network, gas network, and heat network. In [32], the optimal scheduling of microgrids was analyzed in electricity markets considering PtG systems, demand response programs, and energy storage systems. The outputs of these studies also addressed the capability of PtG systems besides demand response and energy storage systems for an efficient demand provision using distributed energy resources.

On the other hand, some other studies focus on improving the resilience of the microgrid. These studies consider the failure of the main grids in different scenarios or use flexible components, such as PtG systems, to reach this aim. For instance, in [33], microgrid operation was optimized under conditions of failure in the main grid that increased load shedding risk. This study introduced a trade-off between resilient and economic operation, as resilient operation increased the operating costs of microgrids. In [34], different outage scenarios were considered for an airport microgrid (e.g., failures of the main grid during peak hours and off-peak hours), and the resiliency of the system considering storage systems and diesel generators was evaluated. It indicated that the integration of storage systems and diesel generators reduced operating costs as well as the duration of network failure in case of an outage. In [35], different scenarios were considered, including grid-connected and islanded ones, to optimize the operation of microgrids to enhance resiliency. This study concluded the proposed approach maximized the profits of microgrids considering the possibility of islanding. In [36], different scenarios for outages in industrial microgrids were taken into consideration in the presence of fuel cells, hydrogen storage tanks, and battery and heat storage systems to improve resiliency. This study demonstrated the use of hydrogen as a backup for generating power and the stochastic scheduling of microgrids to consider outage scenarios reduced load shedding risks. In [37], the role of incentive-based changes in the demand of customers was examined to improve the resiliency of microgrids in islanded mode. It concluded that the flexibility obtained by customers improved the profit of microgrids in both normal and resilient operations. In [38], an unbalanced microgrid was studied considering random variables, such as demand and output power of renewable resources, and examined the resiliency considering contingency constraints that indicated the islanded mode. It concluded the resilient scheduling of microgrids minimized costs and maximized the use of distributed renewable resources. In [39], both failures of the main grid and uncertainty in microgrid resources were considered to enhance resiliency by examining the level of flexibility provided by distributed resources. In [40], the economic mode of operation and a determined resilient mode based on the charge and discharge of energy storage systems were compared in the case of contingency and main grid failure. Based on the results of the reviewed studies, it was necessary to employ a resilient approach using flexibility options to reduce load shedding and provide a technically possible portion of demand when the main grid fails, and microgrids go into islanded mode.

As discussed earlier, solving the optimal operation of microgrids is challenging due to the complexity of the problem, which can be in the form of mixed-integer nonlinear programming (MINLP). Various heuristic methods have been developed to address this problem, such as the Improved Multi-Objective Differential Evolutionary Optimization algorithm [41], an approach based on Differential Evolution and Chaos Theory [42], the Quantum Version of Teaching Learning Based Optimization [43], the Conventional Particle Swarm [44], the Modified Bat Algorithm [45], a Co-Evolutionary algorithm [46], and a hybrid approach based on the Gray Wolf Optimizer, Sine Cosine Algorithm, and Crow Search Algorithm [47]. While heuristic techniques were able to find satisfactory optimal solutions more rapidly using a computational procedure, they often compromised optimality and accuracy. However, a few recent studies focused on the exact methods to solve the optimization problem. For instance, to solve the robust operation of microgrids, a dual Benders Decomposition approach was developed in [48]. The decomposition approach is based on splitting a large optimization problem into smaller subproblems that can be solved independently and combining the results to find a solution to the original problem. Another

Table 1
Systematic review of related work to this study.

Reference	Single-Objective	Multi-Objective	Objectives	Resiliency Consideration			Modeling Approach	Solution Method		Decomposition Approach	Power-to-Hydrogen Systems			
				Failure of the main grid	Flexible components	Another objective		Exact	Heuristic		Gas-to-industry or market	Power-to-gas	Gas-to-power	Gas storage
[15]	✓	–	-Cost minimization	–	–	–	MILP	✓	–	–	–	✓	✓	✓
[16]	✓	–	-Income maximization	–	–	–	MINLP	–	✓	–	–	✓	✓	✓
[17]	–	✓	-Cost minimization -Wind-curtailment minimization	–	–	–	MINLP	–	✓	–	–	✓	✓	✓
[18]	✓	–	-Profit maximization	–	–	–	MILP	✓	–	–	✓	✓	–	–
[19]	✓	–	-Cost minimization	–	–	–	MILP	✓	–	–	–	✓	–	–
[20]	–	✓	-Cost Minimization -Emission minimization	–	–	–	MILP	✓	–	–	–	✓	–	–
[21]	–	✓	-Cost minimization -Emission minimization	–	–	–	MILP	✓	–	–	✓	✓	✓	–
[22]	✓	–	-Cost minimization	–	–	–	MILP	✓	–	–	–	✓	–	✓
[23]	–	✓	-Cost minimization -Emission minimization	–	–	–	MINLP	✓	–	–	✓	✓	✓	–
[24]	✓	–	-Cost minimization	–	–	–	MILP	✓	–	–	✓	✓	–	–
[25]	✓	–	-Cost minimization	–	–	–	MILP	✓	–	–	✓	✓	✓	✓
[26]	✓	–	-Cost minimization	–	–	–	MILP	–	✓	–	✓	✓	–	–
[27]	✓	–	-Cost minimization	–	–	–	MILP	✓	–	–	✓	✓	✓	✓
[28]	✓	–	-Cost minimization	–	–	–	MINLP		✓	–	–	✓	✓	–
[29]	✓	–	-Profit maximization	–	–	–	MILP	–	✓	–	✓	✓	✓	✓
[30]	✓	–	-Cost minimization	–	–	–	MILP	✓	–	–	✓	✓	✓	✓
[31]	✓	–	-Cost minimization	–	–	–	MILP	✓	–	–	✓	✓	✓	✓
[32]	✓	–	-Cost minimization	–	–	–	MILP	✓	–	–	✓	✓	–	✓
[33]	✓	–	-Cost minimization	✓	✓	–	MILP	✓	–	–	–	–	–	–
[34]	✓	–	-Cost minimization	✓	✓	–	MILP	✓	–	–	–	–	–	–
[35]	–	✓	-Cost minimization -Resiliency maximization	✓	✓	✓	MILP	✓	–	–	–	–	–	–
[36]	–	✓	-Cost minimization -Resiliency maximization	✓	✓	✓	MILP	–	✓	SOCR	✓	–	✓	✓
[37]	✓	–	-Cost minimization	✓	✓	–	MILP	✓	–	–	–	–	–	–
[38]	✓	–	-Cost minimization	✓	✓	–	MINLP	✓	–	–	–	–	–	–
[39]	✓	–	-Cost minimization	✓	–	–	MILP	✓	–	–	–	–	–	–
[40]			-Cost minimization -Resiliency maximization	✓	✓	–	MILP	✓	–	–	–	–	–	–
[41]	✓	–	-Cost Minimization	–	–	–	MINLP	–	✓	–	–	–	–	–
[42]	✓	–	-Cost Minimization	–	–	–	MINLP	–	✓	–	–	–	–	–
[43]	✓	–	-Cost Minimization	–	–	–	MILP	–	✓	–	–	–	–	–
[44]	✓	–	-Cost Minimization	–	–	–	MINLP	–	✓	–	–	–	–	–
[45]	✓	–	-Cost Minimization	–	–	–	MINLP	–	✓	–	–	–	–	–
[46]	✓	–	-Cost Minimization	–	–	–	MINLP	–	✓	–	–	–	–	–
[47]	✓	–	-Cost Minimization	–	–	–	MINLP	–	✓	–	–	–	–	–

(*continued on next page*)

Table 1 (*continued*)

Reference	Single-Objective	Multi-Objective	Objectives	Resiliency Consideration			Modeling Approach	Solution Method		Decomposition Approach	Power-to-Hydrogen Systems			
				Failure of the main grid	Flexible components	Another objective		Exact	Heuristic		Gas-to-industry or market	Power-to-gas	Gas-to-power	Gas storage
[48]	✓	–	-Cost Minimization	–	–	–	MINLP	–	✓	–	–	–	–	–
[49]	✓	–	-Cost Minimization	–	–	–	MINLP	✓	–	BD	–	–	–	–
[50]	✓	–	-Cost Minimization	–	–	–	MILP	✓	–	ADMM	–	–		
[51]	✓	–	-Profit maximization of agents	–	–	–	MILP	–	✓	ADMM	✓	✓	✓	✓
Thisresearch	–	✓	-Cost minimization -Resiliency maximization	✓	✓	✓	MINLP	✓	–	GBD	✓	✓	✓	✓

*MILP: Mixed Integer Linear Programming; * MINLP: Mixed Integer Nonlinear Programming; *SOCR: Second Order Conic Relaxation; *BD: Benders Decomposition; *GBD: Generalized Benders Decomposition; *ADMM Alternating Direction Method of Multipliers.

study applied Benders Decomposition to optimize the profit of microgrids during the islanded mode of operation [49]. In [50], a model was proposed to maximize the profit of supply and flexible loads on the demand side in microgrids. This study developed the Alternating Direction Method of Multipliers, which divided the original objective function and constraints to reduce the complexity of the problem like Benders Decomposition. In [51], agent-based scheduling was studied for microgrids considering PtH systems (e.g., electricity and hydrogen systems agents). This study also developed the Alternating Direction Method of Multipliers to solve the optimization problem. It concluded that, in the reviewed studies, the solving methods provided precise solutions benefiting from splitting the problem into smaller subproblems, which decreased complexity compared to solving the original problem.

1.3. Research gaps and contributions

Considering the literature listed above, the comparison of related studies with the proposed approach in this research is given in Table 1. Previous studies have examined the operation of microgrids in the presence of PtH systems, taking into account the conversion of excess electricity to hydrogen and the storage of the hydrogen produced, but the consumption of hydrogen for industrial use has not been fully investigated. Furthermore, the role of PtH systems in enhancing resilience and reducing energy-not-supplied has not been adequately investigated. Nonetheless, current resilience methods primarily focus on failure scenarios of the main grid or the utilization of flexible components like storage systems. Previous studies have not given enough attention to the potential of exact mathematical solutions, such as decomposition methods, in effectively solving the operation model for microgrids in the presence of PtH systems. Given that the problem is formulated as an MINLP problem, exploring these mathematical approaches could yield more accurate solutions.

In view of the above problem, this study proposes a bi-objective model for the resilient operation of industrial microgrids in the presence of PtH systems consisting of electrolyzers, hydrogen storage systems, and fuel cells. In this model, the first objective is the cost of microgrid operation, and the output hydrogen from these systems can either be sold to industry, stored in tanks (i.e., hydrogen storage systems), or consumed to generate electricity using fuel cells. The second objective considers three measures to enhance the resilience of the microgrid by reducing the interaction with the main grid, increasing hydrogen levels in storage systems, and reducing power losses. As the model of resilient operation of microgrids in the presence of PtH systems is bi-objective and in the form of MINLP, a solution approach is developed in which Generalized Benders Decomposition (GBD) is integrated into the Multi-Objective Goal Programming (MOGP) approach. A preprocessing approach is also developed to facilitate the convergence of the solution method. This approach involves two key steps: initializing points for the decomposition method and convexifying the MINLP problem. These steps aim to streamline the optimization process and improve the overall efficiency of the solution approach.

Finally, through the introduction of case studies, various technical analyses are carried out to examine the role of PtH systems in the operation of a microgrid. Analyses are performed with the aim of providing insight into the resilience and economic operation of the microgrid in the presence of PtH systems. The developed solution approach's significance in addressing the complexity of the optimization model for the resilient operation of the microgrid is examined.

1.4. Paper organization

The remainder of this study is structured as follows: In Section 2, an optimization model is proposed for the resilient operation of microgrids considering distributed renewable energy resources, flexible generating units, and PtH systems composed of electrolyzers, hydrogen storage systems, and fuel cells. Subsequently, the solving method is presented,

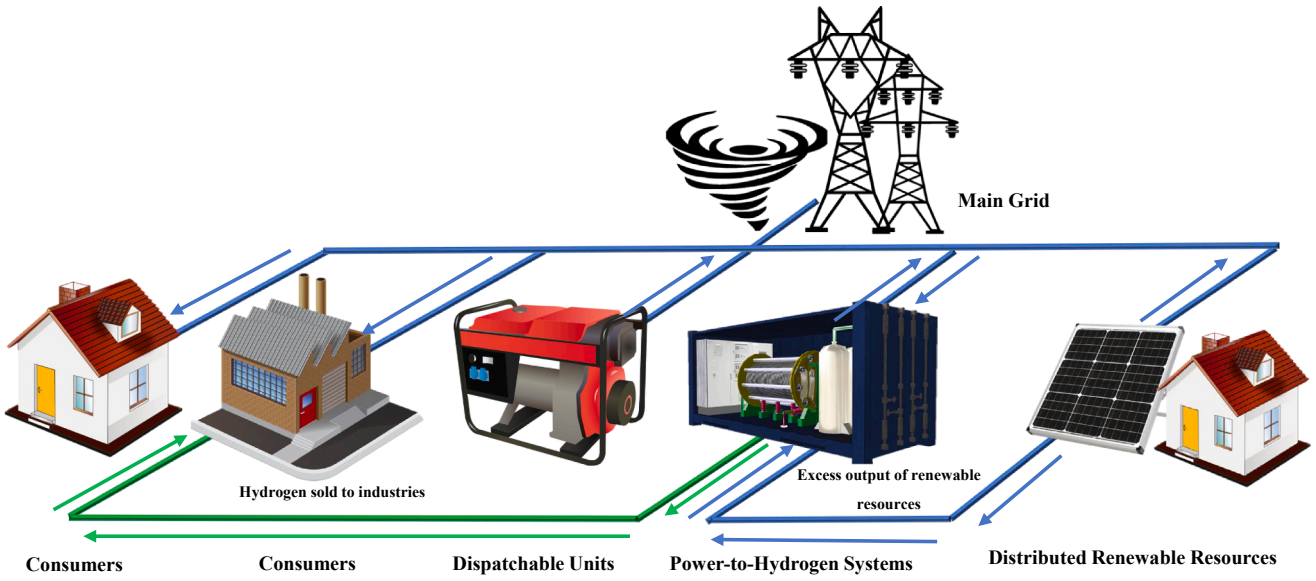

Fig. 1. The illustration of a microgrid connected to the main grid consists of consumers, dispatchable units, PtH systems, and distributed renewable energy resources (blue lines and green lines indicate power flow and hydrogen transmission, respectively). (For interpretation of the references to colour in this figure legend, the reader is referred to the web version of this article.)

which involves combining the MOGP approach with the GBD method. In Section 3, a case study is illustrated to examine the applicability and performance of the proposed model, and an analysis is conducted to assess the effectiveness of the proposed model and provide insights for operators in Section 4. Finally, the main conclusions and future research directions are presented and recapped in Section 5.

2. Model and formulation

A configuration of an industrial microgrid connected to the main grid is illustrated in Fig. 1. As depicted, it consists of consumers, distributed renewable energy resources, flexible natural gas-fired units, and PtH systems. When the output power of distributed energy resources in this microgrid exceeds local demand, the excess power can be consumed by PtH systems' electrolyzers to produce hydrogen from the water. These systems consume electricity to split hydrogen and oxygen from the water through electrolysis. ($2H_2O \rightarrow 2H_2 + O_2$) [52]. In the microgrid, the compressed hydrogen can be either sold to industries or filled into storage tanks of the PtH systems for later use (e.g., generating electricity using PtH systems' fuel cells). Moreover, in the case of any failures in the main grid, the microgrid is disconnected and operated independently in islanded mode. Therefore, it is of significant importance to schedule it considering resilience when any failure in the main grid is predicted. For instance, predicting the level of hydrogen in tanks and being independent of imported power from the main grid could be beneficial as preventive measures when local supply is lower than demand. These measures help local demand provision during a specific period improving the system's resilience.

It should be noted that although the PtH systems, including electrolyzers, hydrogen storage systems, and fuel cells, are cost-intensive, they can be valuable in the scheduling of industrial microgrids from several perspectives. The first one is that hydrogen is necessary for different industries in the area, including metalworking, flats glass production, and electronic industries [53]. Hydrogen sales to industries can provide the operator with revenue that can be used to offset other operating costs. The second one is that these systems are designed to provide the storage capability for excess renewable energy, which can be used during periods of low renewable energy availability or high energy demand. In this way, fuel cells that are used in conjunction with electrolyzers and hydrogen storage systems can be a flexible option to convert hydrogen into power. The last point to consider is that PtH technologies are rapidly advancing, which will improve their efficiency and reduce the costs associated with their deployment [54]. Therefore, the PtH systems can play a key role in achieving decarbonization in the future of energy systems, where all energy needs are met by low/net-zero emission sources.

2.1. Model for the resilient operation of microgrid considering PtH systems

The model for the resilient operation of single-phase and balanced electricity distribution networks of microgrids is indicated in this subsection. It is noteworthy to mention that demand is considered as constant active and reactive power for each hour of operation in the model, and the power loss is also assumed at the beginning of each line. Besides, the microgrid can exchange power with the main grid in electricity markets; hence it is assumed that the day-ahead electricity market was operated to determine electricity price based on the supply and demand (i.e., day-ahead electricity price is determined). In this study, the optimal operation of the microgrids is investigated, meaning all components were previously installed, including PtH systems. The resilient operation of microgrids in the presence of PtH systems is formulated as a bi-objective optimization problem. The reason is that there are two objectives with different scales, including minimizing cost ($) and minimizing de-resilience (kWh). The objective functions and the constraints are explained in the following.

2.1.1. Objective functions

Equation (1) addresses the objective function of the optimal operation of the microgrid considering PtH systems. The objective function consists of five terms: cost of purchasing electricity from the main grid, costs of producing electricity and emissions production using non-

renewable dispatchable units (e.g., microturbines), cost of load shedding, the revenue of selling electricity to the main grid, and revenue of selling hydrogen to industries. It is assumed that the day-ahead electricity market has already been operated, and as a result, the price of electricity has been determined based on the interaction between electricity suppliers and consumers.

$$\text{Minimize } Z_1 = \sum_t \sum_i \delta_{i,t}.P_{i,t}^{buy} + \sum_t \sum_i \left((\alpha_i + \beta_i.\zeta_i).P_{i,t} + \gamma_i.u_{i,t}\right) + \sum_t \sum_i \upsilon_i.P_{i,t}^{lsh} - \sum_t \sum_i \delta_{i,t}^{'}.P_{i,t}^{sell} - \sum_t \sum_c \delta_c^{''}.H_{c,t}^{sell} \quad (1)$$

Three measures are also determined as another objective function to improve the resiliency of the microgrid against predicted events in Eq. (2). More precisely, considering the second objective function improves the operation of the microgrid to be more efficient when it goes to islanded mode. Each term of the objective function is precisely explained in the following.

$$\text{Minimize } Z_2 = \mathscr{R}_1 - \mathscr{R}_2 + \mathscr{R}_3 \quad (2)$$

- *The first term: decrease interactions with the main grid.*

As a resiliency measure, it is necessary to reduce power imports from the main grid (Eq. (3)). The purpose of this measure is to ensure that the microgrid is independent and ensure power supply by locally generated power. When a microgrid operates independently, it can function more reliably in cases of contingency (i.e., in islanded mode).

$$\mathscr{R}_1 = \sum_t \sum_i P_{i,t}^{buy} \quad (3)$$

- *The second term: increase available power through tanks.*

A microgrid can achieve improved operation when the available local supply falls short of demand, if it has sufficient hydrogen supply that can be converted to electricity in the event of contingencies in the main grid. Therefore, the second term of this objective is gas level through tanks multiplied by the efficiency of electricity production, as indicated in Eq. (4).

$$\mathscr{R}_2 = \sum_t \sum_c \varphi_{c,t} HL_{c,t} \quad (4)$$

- *The third term: decrease power loss.*

When the power loss is minimized, consumers are supplied by the nearest suppliers, which improves the reliability of the supply. For this purpose, the third term of the second objective (i.e., the third resiliency measure) is considered to reduce the power loss (Eq. (5)).

$$\mathscr{R}_3 = \sum_t \sum_l R_l.I_{l,t}^2 \quad (5)$$

2.1.1.1. Constraints. In addition to objective functions, constraints of the problem are determined, including active power balance, maximum/minimum output power of renewable and non-renewable generating units, ramp up/down, reactive power balance, Kirchhoff's voltage law and voltage and current limitations, and PtH systems' technical constraints, in the following.

- *Active power balance.*

In Eq. (6), the active power balance for the microgrid is indicated by considering dispatchable and renewable generating units, interactions with the main grid, charge and discharge power of PtH systems, and power loss within the lines [55]. More precisely, it declares that the supply should match the demand in each hour of the operation period [56].

$$P_{i,t} + P_{i,t}^{wind} - P_{c,t}^{E\to H_2} + P_{c,t}^{H_2\to E} + P_{i,t}^{lsh} + P_{i,t}^{buy} - P_{i,t}^{sell} - \sum_{i'} (P_{l,t}^{line} + R_l.I_{l,t}^2) = P_{i,t}^{load} \quad \forall i, \forall l, \forall t \quad (6)$$

- *Maximum/minimum output power of renewable and non-renewable generating units.*

In Eqs. (7)-(8), the maximum/minimum output power of different generating units is demonstrated. The binary variable $u_{i,t}$ represents the status of dispatchable generating units which is equal to one when the units are on and is zero otherwise.

$$P_{i,t}^{wind} \le P_{i,t}^{wind,max} \quad \forall i, \forall t \quad (7)$$

$$u_{i,t}.P_i^{min} \le P_{i,t} \le u_{i,t}.P_i^{max} \quad \forall i, \forall t \quad (8)$$

- *Ramp up/down.*

In Eqs. (9)-(10), the ramp-up and ramp-down constraints of dispatchable generating units are indicated, which refers to their capability to change their output power. A fast ramping rate capability is appropriate to deal with the variable output power of renewable generating units, called flexibility measure.

$$P_{i,t} - P_{i,t-1} \le R_i^{maxup} \quad \forall i, \forall t \quad (9)$$

$$P_{i,t-1} - P_{i,t} \le R_i^{maxdown} \quad \forall i, \forall t \quad (10)$$

- *Reactive power balance.*

In Eq. (11), the reactive power balance in the network is presented.

$$Q_{i,t} + Q_{i,t}^{wind} + \sum_{i'} (Q_{l,t}^{line} + X_l.I_{l,t}^2) = Q_{b,t}^{load} \quad \forall i, \forall l, \forall t \quad (11)$$

- Kirchhoff's voltage law and voltage & current limitations.

In Eqs. (12)-(13), Kirchhoff's voltage law for each time step is indicated [57]. Eqs. (14)-(15) indicate the voltage limitation at each node and the current limitation through each line.

$$V_{l,t}^{in\,2} - V_{l,t}^{out\,2} = 2\left(R_l.P_{l,t}^{line} + X_l.Q_{l,t}^{line}\right) + Z_l^2.I_{l,t}^2 \quad \forall l, \forall t \quad (12)$$

$$V_{l,t}^2.I_{l,t}^2 = Q_{l,t}^{line2} + P_{l,t}^{line2} \quad \forall l, \forall t \quad (13)$$

$$V_i^{min} \le V_{i,t} \le V_i^{max} \quad \forall i, \forall t \quad (14)$$

$$\left|I_{l,t}\right| \le I_l^{max} \quad \forall l, \forall t \quad (15)$$

- *PtH systems' technical constraints.*

In Eqs. (16)-(20), constraints are indicated related to the operation of PtH systems in microgrids. According to Eq. (16), excess power from a microgrid ($P_{c,t}^{E\to H_2}$) can be used to produce hydrogen utilizing electrolyzers. Hydrogen produced ($H_{c,t}^{in}$) is compressed and stored within tanks, as indicated in Eq. (17). It should be noted that, in this equation, the stored amount of hydrogen from the previous operating period is also taken into consideration (HL_c^0). More precisely, the amount of hydrogen stored within tanks at the end of each operating period will be used as the initial amount at the beginning of the next operating period. The stored amount of hydrogen can either be used in generating electricity

for later uses by fuel cells ($H^{E}_{c,t}$) or sold for use in other industries ($H^{sell}_{c,t}$), as indicated in Eqs. (18)-(19). Additionally, Eq. (20) indicates the level of hydrogen stored within the tanks ($HL_{c,t}$) cannot exceed its maximum ($HL^{max}_{c,t}$). The discharge of hydrogen to produce electricity in microgrids and the sale of hydrogen to industries are also limited by Eqs. (21)-(22). Binary variables are also defined ($\rho_{c,t}$ and $\varrho_{c,t}$), and another constraint is introduced to prevent that each storage can be discharged to produce electricity in the microgrid and supply industries, simultaneously (Eq. (23)). The reason is that fuel cells need hydrogen at a specific pressure to operate efficiently. Therefore, the simultaneous discharge of hydrogen from storage systems should be avoided so that fuel cells can operate properly [58,59].

$$P^{E\to H_2}_{c,t}\rho_{c,t} = H^{in}_{c,t} \quad \forall c, \forall t \tag{16}$$

$$HL_{c,t} = \begin{cases} HL^{0}_{c} \quad if \quad \forall c, t = 1 \\ HL_{c,t-1} + \left(\phi_c.H^{in}_{c,t} - \dfrac{H^{out}_{c,t}}{\varphi_c}\right) \quad if \quad \forall c, \forall t \geq 2 \end{cases} \tag{17}$$

$$H^{out}_{c,t} = H^{E}_{c,t} + H^{sell}_{c,t} \quad \forall c, \forall t \tag{18}$$

$$H^{E}_{c,t}.\psi_c = P^{H_2\to E}_{c,t} \quad \forall c, \forall t \tag{19}$$

$$HL_{c,t} \leq HL^{max}_{c,t} \quad \forall c, \forall t \tag{20}$$

$$H^{E}_{c,t} \leq \rho_{c,t}.HL^{maxE}_{c,t} \quad \forall c, \forall t \tag{21}$$

$$H^{sell}_{c,t} \leq \varrho_{c,t}.HL^{maxsell}_{c,t} \quad \forall c, \forall t \tag{22}$$

$$\rho_{c,t} + \varrho_{c,t} \leq 1 \quad \forall c, \forall t \tag{23}$$

2.2. Solving approach based on GBD and MOGP

To address the resilient operation of microgrids with PtH systems, a solving method is devised that combines the GBD technique with the MOGP approach. This combination provides an effective solution for optimizing microgrid operations under various scenarios and enables efficient utilization of PtH systems. An upside to the MOGP method is the reduction in the number of iterations and solving time of the MINLP model [60]. Different satisfaction levels for each objective function can be considered using MOGP to provide insights for the operators. The first step of the MOGP is to calculate the positive ideal and negative ideal solutions for each objective function. After that, using the obtained results in the last step, membership functions are determined for the objective functions. In the third step, the weighted sum of objective functions is optimized to find the maximum level of satisfaction of constraints for each objective. Finally, MOGP is added as a constraint, and the model is solved iteratively, which provides a set of solutions to be opted by operators. However, to solve the resilient operation of microgrids in the presence of PtH systems using the four-step MOGP approach, the problem contains binary variables and nonlinear constraints, which makes the model an MINLP problem. To handle this issue, an approach based on Benders Decomposition, called GBD, is combined with the MOGP method for solving this MINLP problem. Proposed a few decades ago [61,62], GBD has often been employed to solve optimization problems in different fields, such as telecommunication, energy, and transport. As non-convexity is often associated with MINLP problems, within a finite number of iterations, the GBD fixes the non-convexity problem and converges to the exact solution [49,50]. Therefore, this approach is an appropriate option to optimize the resilient operation of microgrids due to the nonlinear constraints (Eqs. (12)-(13)) and binary decision variable ($u_{i,t}$, $\rho_{c,t}$, and $\varrho_{c,t}$).

In the following, at first, the main step of the MOGP method to solve the problem of resilient operation of microgrids in the presence of PtH systems is determined step-by-step. Then, it is explained how the GBD method is integrated into the MOGP method to solve the optimization problem.

- *MOGP: the first step.*

The first step involves finding ideal and non-ideal solutions by solving the optimization problem considering only one of the objective functions and ignoring the other one at any time [63]. For instance, in Eqs. (24), minimizing the first objective function provide an ideal and a non-ideal solution for the resilient operation of microgrids in the presence of PtH systems (Z^{+}_{1} and Z^{-}_{2}, respectively (Eq. (25)). In Eq. (26), the other ideal and non-ideal solutions are also determined for the problem studied (Z^{+}_{2} and Z^{-}_{1}, respectively (Eq. (27)). More precisely, when the optimization problem is solved by considering only one objective function, it provides an ideal solution for that objective function and a non-ideal solution for the other objective function.

$$\begin{aligned} &\text{Minimize } Z_1 \\ &\text{Subject to} \\ &\text{Equations } (6)-(23) \end{aligned} \tag{24}$$

$$Z^{+}_{1} = Z^{*}_{1} \text{ and } Z^{-}_{2} = Z^{*}_{2} \tag{25}$$

$$\begin{aligned} &\text{Minimize } Z_2 \\ &\text{Subject to} \\ &\text{Equations } (6)-(23) \end{aligned} \tag{26}$$

$$Z^{+}_{2} = Z^{*}_{2} \text{ and } Z^{-}_{1} = Z^{*}_{1} \tag{27}$$

- *MOGP: the second step*

A membership function (ψ_1 and ψ_2) is determined for each objective function as indicated in Eq. (28). In this way, the membership functions are determined for the problem of the resilient operation of the microgrids.

$$\psi_1 = \begin{cases} 1 & if \ \ Z_1 \leq Z^{+}_{1} \\ \dfrac{Z^{-}_{1} - Z_1}{Z^{-}_{1} - Z^{+}_{1}} & if \ \ Z^{-}_{1} \leq Z_1 \leq Z^{+}_{1} \\ 0 & if \ \ Z_1 \geq Z^{-}_{1} \end{cases}$$

$$\psi_2 = \begin{cases} 1 & if \ \ Z_2 \leq Z^{+}_{2} \\ \dfrac{Z^{-}_{2} - Z_2}{Z^{-}_{2} - Z^{+}_{2}} & if \ \ Z^{-}_{2} \leq Z_2 \leq Z^{+}_{2} \\ 0 & if \ \ Z_2 \geq Z^{-}_{2} \end{cases} \tag{28}$$

- *MOGP: the third step*

A maximum level of satisfaction for the constraints is determined by solving a crisp model indicated in Eq. (29). In the optimization problem, ς, ω_h, and h respectively indicate the maximum level of satisfaction for the constraints, weighted coefficients ($\sum_h \omega_h = 1$) determined by decision-makers (i.e., microgrid operator in the problem of resilient operation of microgrids), and a set of objective functions.

$$\begin{aligned} &\text{Maximize} \sum_h \omega_h \varsigma_h \\ &\text{subject to} \\ &\psi_h \geq \varsigma \quad h = 1 \text{ and } 2, \ \varsigma \in [0,1] \\ &\text{Equations } (6)\text{–}(23) \end{aligned} \tag{29}$$

- *MOGP: the fourth step*

Table 2
Main steps of GBD to solve an MINLP optimization problem.

Loop
Initialization
$Iteration := 1$
$Upperbound = \infty$
Initializing binary variables $y^{(k)}$
The first step: nonlinear programming subproblem
Minimize $Z^{primal} = C^T y^{(k)} + f(x)$
Subject to
$h(x) = 0,\ g(x) \le 0,\ Cx + By^{(k)} \le b,\ Ay \le \alpha, x \in R^n$
The solutions are optimal multipliers ($\lambda^{(k)}$) and decision variable ($x^{(k)}$)
if $Z^{primal} \le Upperbound$
$Upperbound := Z^{primal}$
$\lambda^{new} := \lambda^{(k)}$
$x^{new} := x^{(k)}$
End
The second step: mixed integer programming master problem
Minimize $Z^{master} = \mu$
Subject to
$\mu \ge C^T y + f(x^k) - \lambda^{(k)}(C^T x^{(k)} + By - b)$
$Ay \le \alpha,$
$y \in \{0,1\}$
The solution is $y^{(k+1)}$
The third step: convergence checking
If $Z^{master} \ge Upperbound$
Stop
Else
$Iteration := Iteration + 1$
Go to step 1
End

Finally, goal programming is integrated into the approach to solving the resilient operation of microgrids by adding a constraint ($\psi_h^{new} \ge \psi_h$) into the model proposed in the last step (Eq. (30)). This step is repeated until it provides an appropriate level of satisfaction (ζ) for the microgrid operator. Meanwhile, an analysis of weighted coefficients is carried out by modifying the weights assigned to each objective function. This analysis aims to provide decision-makers with valuable insights by exploring the impact of different weightings on the overall optimization results.

$$\begin{aligned} &\text{Maximize} \sum_h \omega_h \zeta_h \\ &\text{subject to} \\ &\psi_h \ge \zeta_h \quad h = 1 \text{ and } 2, \zeta_h \in [0,1] \\ &\psi_h^{new} \ge \psi_h \\ &\text{Equations (6)–(23)} \end{aligned} \tag{30}$$

Despite using the MOGP approach to solve the bi-objective problem presented in this study, challenges remain in solving the Mixed-Integer Nonlinear Programming (MINLP) problems encountered in the first, third, and fourth steps. For this purpose, GBD is integrated into the MOGP to cope with this issue. The concept of GBD is to solve the primal problem first and then the master problem, which generates an upper bound and a lower bound. Firstly, the primal problem is solved by initializing the binary variables in the first iteration that provides the upper bound and Lagrange Multipliers related to constraints. After that, the master problem is determined by employing duality theory and Lagrange Multipliers of the previous step. The solution to the master problem provides a lower bound and binary variable for the next iteration. The procedure converges in a finite number of iterations when the upper bound is greater or equal to the lower bound. Considering an MINLP problem in the form of Eq. (31), the main steps of this decomposition approach are represented in detail in Table 2.

Table 3
Main steps of GBD to solve the resilient operation of microgrids in the presence of PtH systems.

Loop
Initialization
$Iteration := 1$
$Upperbound = \infty$
Initializing binary variables $u_{i,t}^{(k)}, \rho_{c,t}^{(k)}$, and $\varrho_{c,t}^{(k)}$
The first step: nonlinear programming subproblem
Minimize $Z^{primal} = \sum_t\sum_i(\gamma_i.u_{i,t}^{(k)}) + \sum_t\sum_i \delta_{i,t}.P_{i,t}^{buy} + \sum_t\sum_i((\alpha_i + \beta_i.\zeta_i).P_{i,t}) + \sum_t\sum_i v_i.P_{i,t}^{lsh} - \sum_t\sum_i \delta_{i,t}^{'}.P_{i,t}^{sell} - \sum_t\sum_c \delta_{c,t}^{''}.H_{c,t}^{sell}$
Subject to
Equations (6), (7), (9), (10), (11), (12), (13), (14), (15), (16), (17), (18), (19), and (20)
$u_{i,t}^{(k)}.P_i^{min} \le P_{i,t} \le u_{i,t}^{(k)}.P_i^{max}, \mathscr{L}_{i,t}^{(k)}, \mathscr{L}'^{(k)}_{i,t}, \forall i, \forall t$
$H_{c,t}^{E} \le \rho_{c,t}^{(k)}.HL_{c,t}^{maxE}$
$\mathscr{G}_{c,t}^{(k)}, \forall c, \forall t$
$H_{c,t}^{sell} \le \varrho_{c,t}^{(k)}.HL_{c,t}^{maxsell}, \mathscr{R}_{c,t}^{(k)}, \forall c, \forall t$
$\rho_{c,t}^{(k)} + \varrho_{c,t}^{(k)} \le 1, \varkappa_{c,t}^{(k)}, \forall c, \forall t$
The solutions are optimal multipliers of constraints and continuous decision variables
if $Z^{primal} \le Upperbound$
$Upperbound := Z^{primal}$
$P_{i,t}^{buy^{new}} := P_{i,t}^{buy^{(k)}}$
$P_{i,t}^{new} := P_{i,t}^{(k)}$
$P_{i,t}^{lsh^{new}} := P_{i,t}^{lsh^{(k)}}$
$P_{i,t}^{sell^{new}} := P_{i,t}^{sell^{(k)}}$
$H_{c,t}^{sell^{new}} := H_{c,t}^{sell^{(k)}}$
and…
$\mathscr{L}^{new} := \mathscr{L}_{i,t}^{(k)}$
$\mathscr{L}'^{new} := \mathscr{L}'^{(k)}_{i,t}$
$\mathscr{G}^{new} := \mathscr{G}_{c,t}^{(k)}$
$\mathscr{M}^{new} := \mathscr{M}_{c,t}^{(k)}$
End
The second step: mixed integer programming master problem
Minimize $Z^{master} = \mu$
Subject to
$\mu \ge \sum_t\sum_i(\gamma_i.u_{i,t}^{(k)}) + \sum_t\sum_i \delta_{i,t}.P_{i,t}^{buy^{(k)}} + \sum_t\sum_i((\alpha_i + \beta_i.\zeta_i).P_{i,t}^{(k)}) + \sum_t\sum_i v_i.P_{i,t}^{lsh^{(k)}} - \sum_t\sum_i \delta_{i,t}^{'}.P_{i,t}^{sell^{(k)}} - \sum_t\sum_c \delta_{c,t}^{''}.H_{c,t}^{sell^{(k)}} + \sum_t\sum_i \mathscr{L}'^{(k)}_{i,t}.(P_{i,t}^{(k)} - u_{i,t}.P_i^{max}) + \sum_t\sum_c \mathscr{G}_{c,t}^{(k)}.(H_{c,t}^{E(k)} - \rho_{c,t}.HL_{c,t}^{maxE}) + \sum_t\sum_c \mathscr{R}_{c,t}^{(k)}.(H_{c,t}^{sell(k)} - \varrho_{c,t}.HL_{c,t}^{maxsell});$
$\rho_{c,t} + \varrho_{c,t} \le 1$
$u_{i,t}, \rho_{c,t},$ and $\varrho_{c,t} \in \{0,1\}$
The solutions are $u_{i,t}^{(k+1)}, \rho_{c,t}^{(k+1)},$ and $\varrho_{c,t}^{(k+1)}$
The third step: convergence checking
If $Z^{master} \ge Upperbound$
Stop
Else
$Iteration := Iteration + 1$
Go to step 1
End

$$\begin{aligned} &\text{Minimize } C^T y + f(x) \\ &\text{Subject to} \\ &h(x) = 0,\ g(x) \le 0,\ Cx + By \le b \\ &x \in R^n,\ y \in \{0,1\} \end{aligned} \tag{31}$$

As demonstrated, initialization of iteration ($Iteration := 1$), upper bound ($Upperbound = \infty$), and binary variables ($y^{(k)}$) are implemented, and after that, the primal problem is solved in the form of nonlinear programming (i.e., the first step). The output of solving the primal problem provides an upper bound ($Upperbound := Z^{primal}$), Lagrange Multipliers ($\lambda^{(k)}$), and continuous variables ($x^{(k)}$) for the next step. In the second step, the master problem is solved, as demonstrated in the above table (i.e., the second step). The third step is also convergence checking

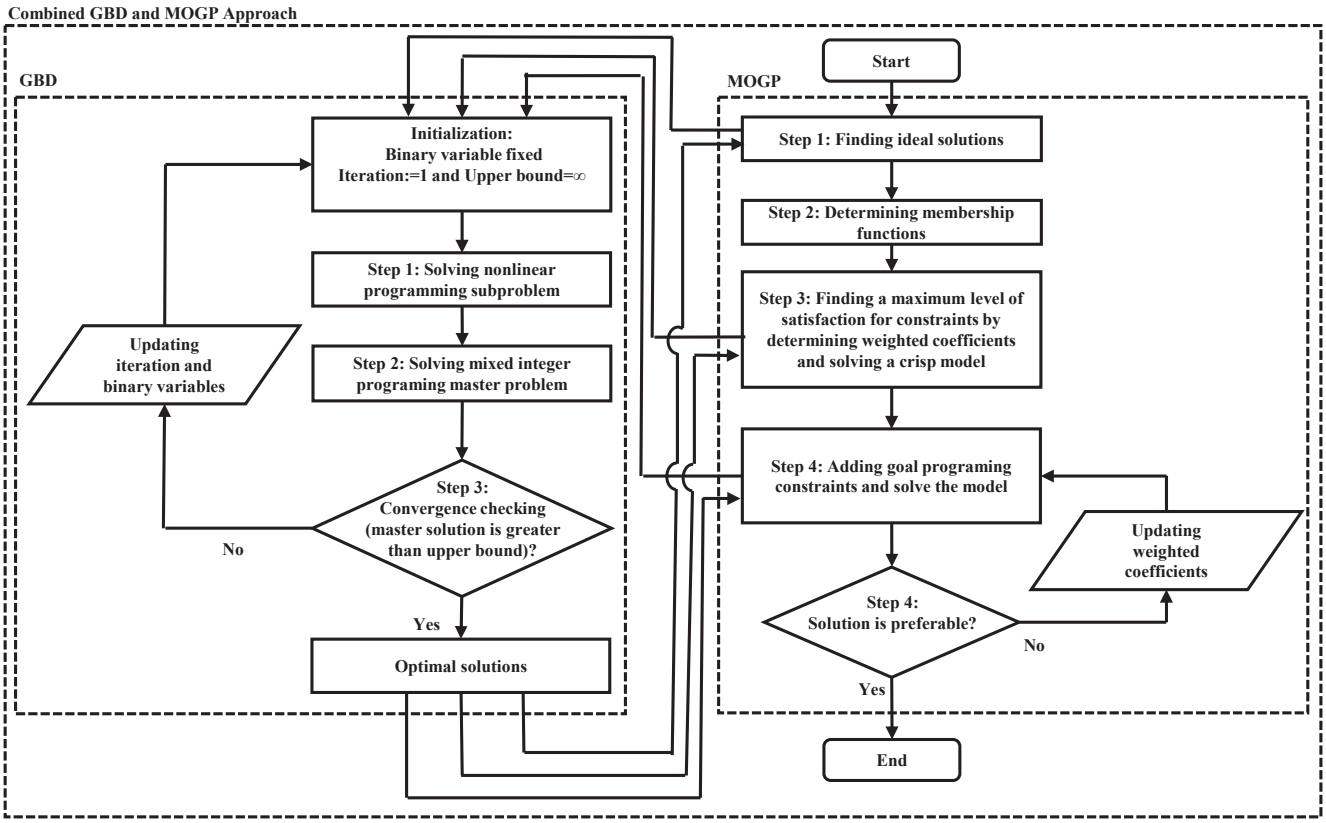

Fig. 2. Main steps of the developed solving approach to optimize the resilient operation of microgrids in the presence of PtH systems.

($Z^{master} \geq Upperbound$) and updating iteration ($Iteration := Iteration + 1$) when another iteration is required. As an example, in Table 3, the main steps of this decomposition approach to solve the operation of PtH systems in microgrids are demonstrated (i.e., solving the optimization problem discussed at the first step of MOGP (Eq. (24)).

Fig. 2 illustrates the main stages involved in solving the resilient operation of microgrids with PtH systems using the developed solving approach. More precisely, this figure indicates the flowchart of solving the optimization problem using the developed approach. As depicted, on the right side of the figure, the main steps of MOGP are demonstrated as discussed previously. Based on this approach, in the first, third, and fourth steps of the MOGP approach, the GBD method is integrated to solve the optimization problems, indicated on the left side of the figure, as discussed earlier (See Fig. 3.)

It should be noted that the model is non-convex in its current form, which means that the solution method may lead to local optimum solutions. While GBD is an appropriate solving method to deal with the MINLP problem, a pre-processing technique could help to achieve a unique solution. The first step of this technique is to prepare the optimization problem by reformulating Eq. (13) into Eq. (32), which transforms the non-convex optimization problem of optimal power flow into a convex one by a conic program based on [64]. More precisely, by converting the model into a convex optimization problem, achieving a unique solution is guaranteed. The second step of pre-processing is to solve the relaxed optimization problems in which binary variables are considered as continuous variables between zero and one. After solving the relaxed problem, initial points for solving the original problem using GBD are obtained by rounding the value of these continuous variables. As a result, this method prevents initializing the binary variable inappropriately. The third step of this method is based on adding slack variables to the power flow balance equation (Eq. (33)), adding the corresponding considerable penalty to the objective function (Eq. (34)), and solving the obtained optimization problem. It also prevents trapping into local optimum or infeasible solutions by overestimating the feasible region, as demonstrated in Fig. 4 [65]. The main reason is that the initializing binary variable may still lead to infeasible solutions in the early iterations of the proposed solving approach. Although the third step assists in coping with the problem, the value of the slack variable must be zero if a unique solution is to be obtained. On the other hand, the initial points and penalties must be updated to reach this aim [66].

$$V_{l,t}^{2}.I_{l,t}^{2} \geq Q_{l,t}^{line2} + P_{l,t}^{line2} \quad \forall l, \forall t \tag{32}$$

$$P_{i,t} + P_{i,t}^{wind} - P_{c,t}^{E\rightarrow H_2} + P_{c,t}^{H_2\rightarrow E} + P_{i,t}^{lsh} + P_{i,t}^{buy} - P_{i,t}^{sell} - \sum_{i}(P_{l,t}^{line} + R_l.I_{l,t}^{2}) + SV_{i,t}^{s} = P_{i,t}^{load} + SV_{i,t}^{d} \quad \forall i, \forall l, \forall t \tag{33}$$

$$Z^{'} = Z + \sum_{t}\sum_{i} PN.(SV_{i,t}^{s} + SV_{i,t}^{d}) \tag{34}$$

It should be noted that, as this study examines the resilience operation of microgrids in the presence of PtH systems, developing the method based on the decomposition provide more accurate solutions in comparison with linearization. The reason is that the linearization techniques are an approximation around specific points and provide a less accurate solution when the distance from the points increases [67,68]. Therefore, in this case, applying the GBD method leads to a more accurate solution and guarantees a globally optimal solution.

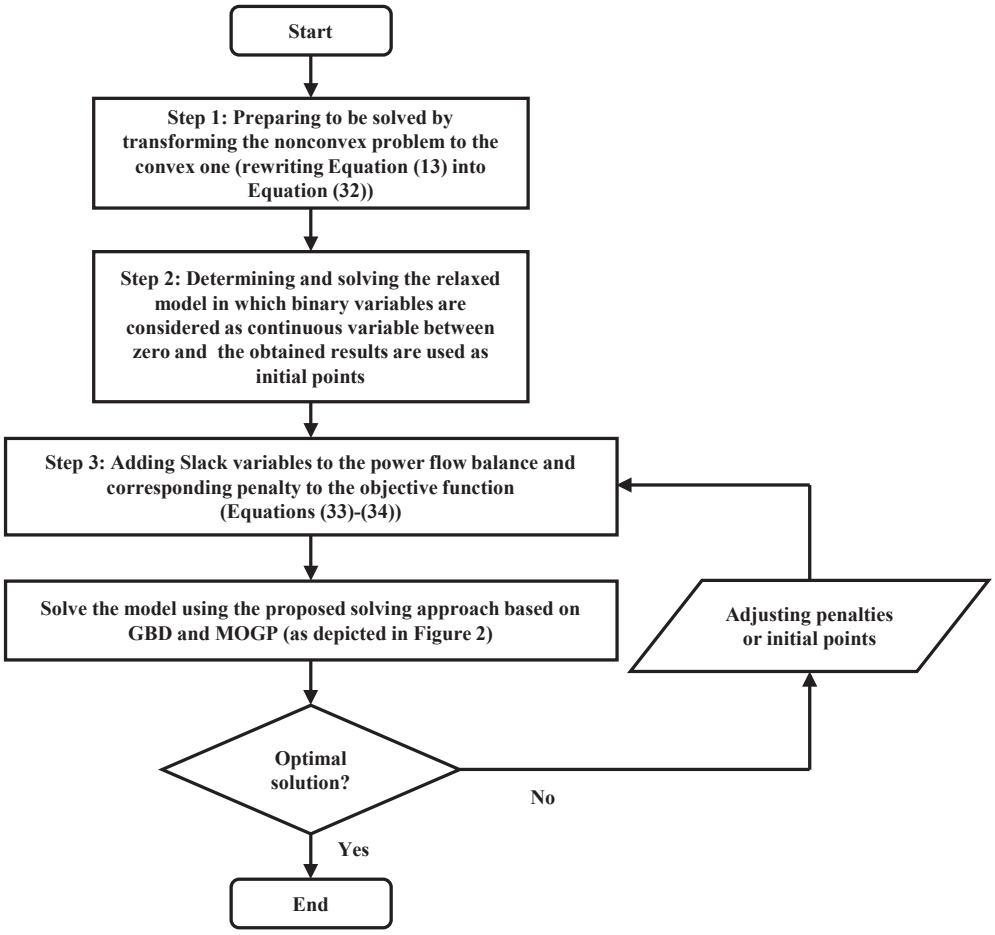

Fig. 3. Main steps of the developed preprocessing approach to optimize the resilient operation of microgrids in the presence of PtH systems.

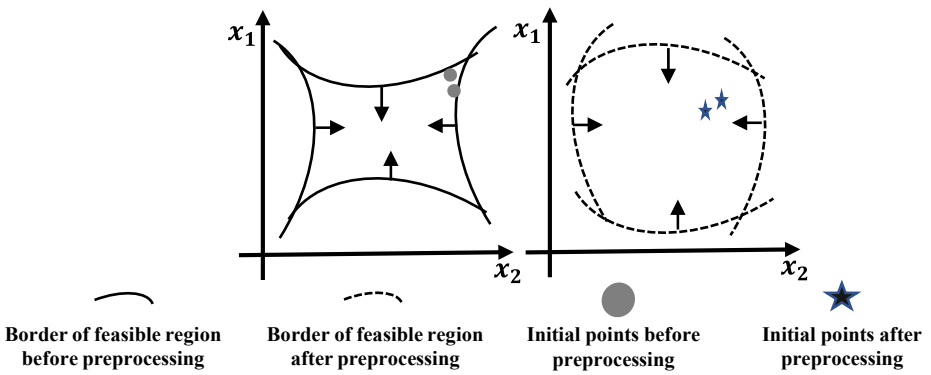

Fig. 4. Feasible solution and initial points for the solving method with and without preprocessing.

3. Case study

In this study, based on real-world data, an industrial microgrid is taken into consideration to analyze the role of PtH systems, the resiliency consideration approach, and the solving approach from technical and economic aspects. As depicted in Fig. 5, a microgrid is studied, which consists of 33-node, 32-line, four connections to wind generators, three connections to PtH systems, and two connections to dispatchable units. In a normal situation, the microgrid can sell/buy electricity to/from the main grid. While the microgrid is connected to the main grid in the normal operation mode, in case of a contingency in the main grid (e.g., equipment failure caused by severe weather), this microgrid operates independently in the islanded mode.

It is worthwhile to mention that, in the paper, PtH systems are examined that consist of alkaline electrolysis technology, known for its robustness and long-standing presence in the industry [69].

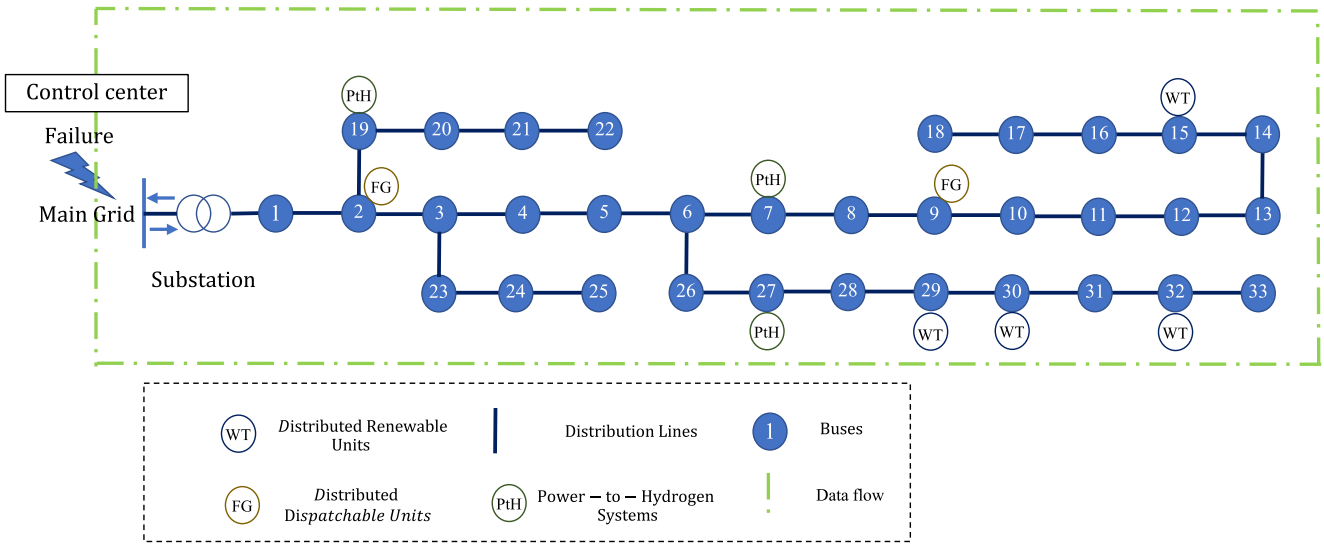

Fig. 5. Illustration of the microgrid examined in this study, including PtH systems, dispatchable units, and distributed renewable resources.

Table 4
Characteristics of different systems installed in the microgrid.

System	Location	Installed capacity	Characteristics of each unit
Windturbines	Node 15, Node 29, Node 30, and Node 32	2400 kW	$P_{i,t}^{wind,max} = 600$ kW
Dispatchable units	Node 9	100 kW	$\alpha_i = 0.04$ \$/kW, $P_i^{min} = 10$ kW, $P_i^{max} = 100$ kW, $R_i^{maxup/down} = 50$ kW, $\beta_i = 5$ \$/Ton, and $\zeta_i = 0.0003$ Ton/kW
Dispatchable units	Node 2	500 kW	$\alpha_i = 0.25$ \$/kW, $P_i^{min} = 100$ kW, $\beta_i = 65$ \$/Ton, and $P_i^{max} = 500$ kW, $\zeta_i = 0.000417$ Ton/kWh [72] $R_i^{maxup/down} = 125$ kW,
PtH systems	Node 7, Node 19, and Node 27	1200 kW	$\phi_c = 60\%$, $\varphi_c = 36\%$, $HL_{c,t}^{max} = 2000\,m^3$, and $\delta_c^{'} = 6\$/m^3$

Table 5
Scenarios examined in the study.

No.	Scenario	Further explanations
1	Different prices of hydrogen	• 100 %, 10 %, and 1 % of real prices of hydrogen
2	Distributed PtH systems and a centralized PtH system	• Centralized PtH system capacity is equal to the sum of distributed PtH systems Centralized PtH system is connected to node 7
3	No PtH systems	
4	Low wind availability	• 20 % wind availability Hydrogen storage full at the start of the operating period

Additionally, proton exchange membrane (PEM) fuel cells are integrated to convert the stored hydrogen back into electricity, with the added benefit of a fast start-up time, albeit with a higher cost due to the required catalyst [70]. The produced hydrogen is also compressed to be stored in steel-made cylinders under high pressure. By combining these technologies, PtH systems can transform surplus electrical energy into a storable and versatile form of fuel that can be utilized for power generation or in various industrial applications.

In Table 4, the location, capacity, and characteristics of the components installed in this microgrid are addressed [71]. All required data to simulate the electricity network in the microgrid are also presented in Appendix.

Considering the case study, different scenarios are investigated (Table 5), including various prices of hydrogen (Scenario 1), a centralized PtH system versus distributed PtH systems (Scenario 2), no PtH systems (Scenario 3), and a low wind power availability, as an example of extreme weather events (Scenario 4). It should be noted that the proposed model for the resilient operation of microgrids in the presence of PtH systems is implemented in General Algebraic Modeling System (GAMS) using a computer with an Intel Core i8 processor and 8 GB of RAM.

4. Result and analysis

The results and analyses presented in this section are divided into two main subsections. The role of PtH systems is examined in the operation of the microgrid from technical and economic viewpoints in Subsection 4.1 (Scenario 1 and Scenario 2). In Subsection 4.2, the role of the resiliency consideration approach to mitigate load shedding in the microgrid is examined along with the output of the developed approach to solve the optimization problem (Scenario 3 and Scenario 4).

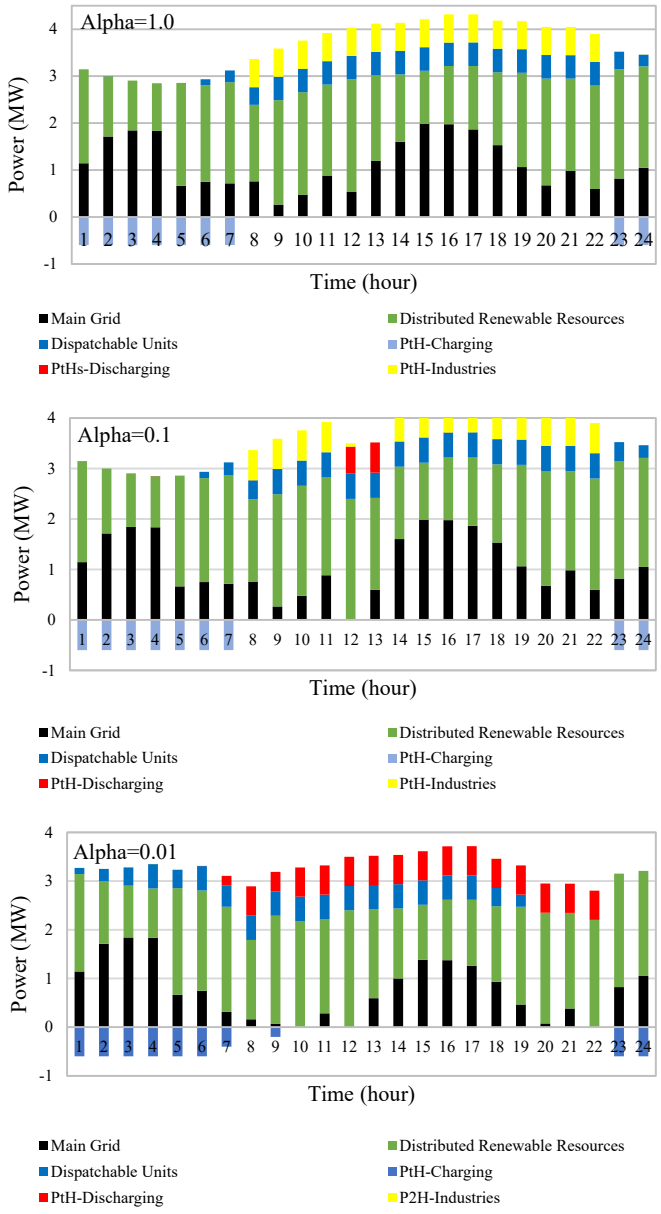

Fig. 6. Examining the scheduling of the microgrid considering different prices for hydrogen during normal operation.

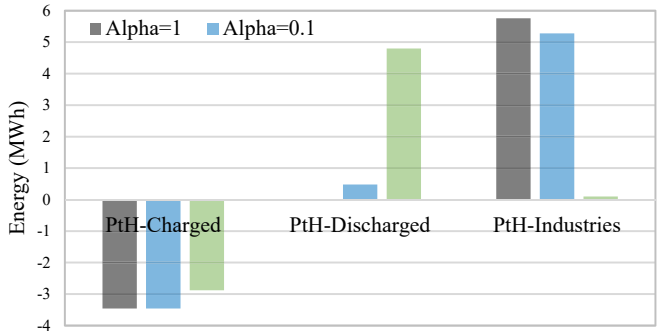

Fig. 7. Charge and discharge of PtH systems in the microgrid.

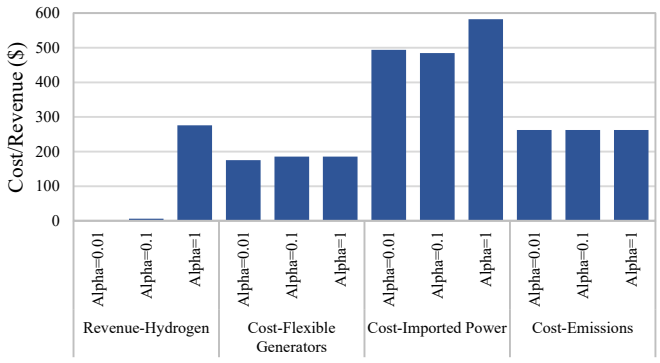

Fig. 8. Different terms of the first objective function considering various prices for hydrogen during normal operation.

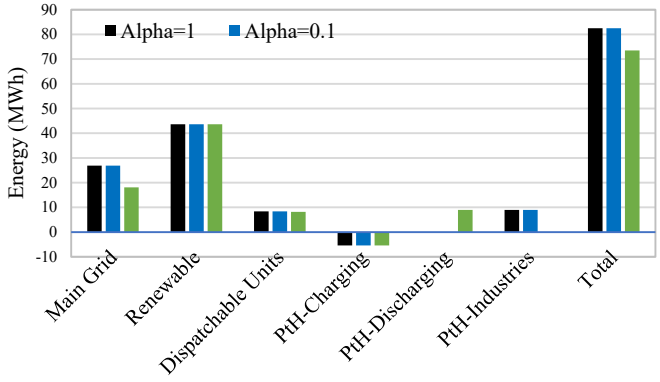

Fig. 9. Energy supply in the microgrid.

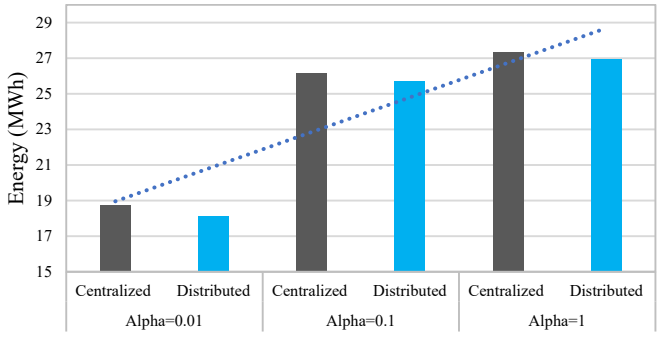

Fig. 10. Imported power from the main grid- a centralized PtH system versus distributed PtH systems.

4.1. PtH systems techno-economic analysis

In this subsection, firstly, an analysis is conducted to examine the optimal operation of the microgrid versus different hydrogen prices (i.e., Scenario 1). The main reason is that the price of hydrogen is decreasing

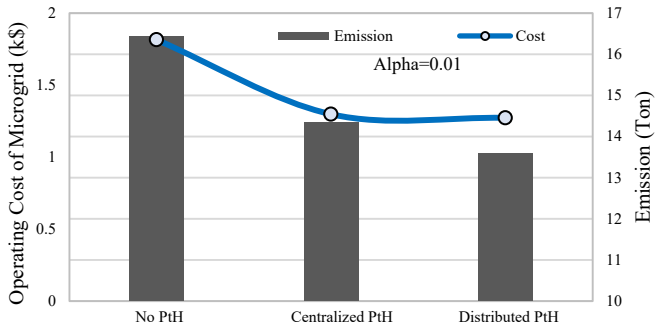

Fig. 11. Operating cost of microgrid versus the produced amount of emissions.

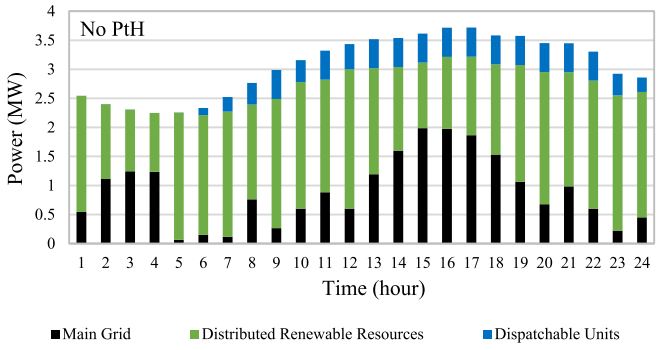

Fig. 12. Scheduling of microgrid without PtH systems.

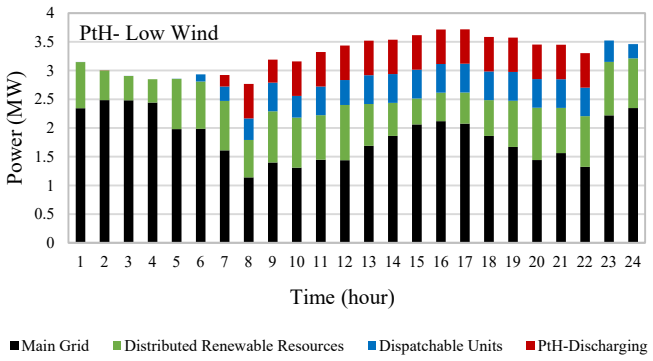

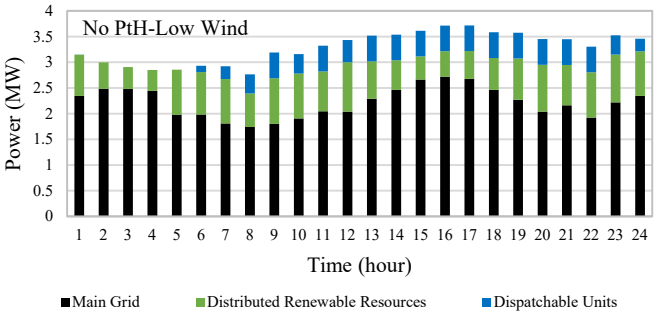

Fig. 13. Scheduling of microgrid when low wind power is available in the presence and absence of PtH systems.

mainly due to improvements in production technologies, the promotion of the use of renewable resources, and government policies to use clean energy. For this purpose, the output and/or input power of different components as well as interactions with the main grid are illustrated in Fig. 6. It demonstrates that the excess electricity in the microgrid is converted to hydrogen during off-peak hours of operation (from 00:00 to 07:00 and from 23:00 to 24:00), and the amount of stored hydrogen within tanks of PtH systems is used for either electricity production or industries' demand provision during peak hours of operation (from 08:00 to 22:00). When the price of hydrogen is high, the stored hydrogen within tanks is continuously sold to industries (Alpha = 1.0). Examination of a low price of hydrogen shows that, in this case, the stored hydrogen is persistently converted to electricity to supply peak demand (Alpha = 0.01). However, when Alpha is equal to 0.1, only at the beginning of peak hours, the stored hydrogen is converted to electricity, and it is mostly used to supply the required amount of hydrogen for industries.

Fig. 7 further illustrates the total charged and discharged energy of the PtH systems as part of the overall solving approach for the resilient operation of microgrids. It shows that the charged energy is less than 4 MWh, and the PtH systems are discharged either to provide hydrogen for industry or supply energy in the microgrid according to the price of hydrogen. However, in the case of high hydrogen prices, the hydrogen sold to the industry is much higher than in other cases. It is due to a substantial revenue stream from hydrogen sales at high prices, which makes importing power from the main grid and converting it into hydrogen using PtH systems a beneficial option. It is supported by an illustration of different terms of the first objective function for different prices of hydrogen, indicated in Fig. 8. This figure indicates the revenue of selling hydrogen to industry, the cost of imported power from the main grid, the cost of emission, and the cost of flexible generating units operation. Based on the examination, when the price of hydrogen is high, the cost of imported power from the main grid is high as converting to hydrogen and selling to industry provides a significant revenue that offsets a portion of operating costs.

In Fig. 9, the total imported and exported energy to/from the microgrid is also illustrated, including imported energy from the main grid, supplied energy by renewable and dispatchable systems, and charged and discharged energy of PtH systems. It indicates that renewable energy sources provide a substantial portion of electricity demand (about 40 MWh). However, the main grid still provides about 20 MWh of electricity demand. The flexible generating units only supply the electricity demand during peak hours. Due to the lower price of the main grid compared to the operating costs of flexible generating units (i.e., based on Table 9 and Table 4), imported power from the grid is given priority over flexible generating units. Due to the technology of dispatchable units connected to node 2, the variable cost of operation is 0.25 $/kWh, while the maximum price of electricity is 0.16 $/kWh. For resilient operations, however, dispatchable units in the microgrid would supply the energy to minimize dependence on the main grid.

To analyze the role of PtH systems, another examination is also conducted that compares the operation of distributed against centralized PtH systems in this microgrid (i.e., Scenario 2). It is worthwhile to mention that the capacity of the centralized PtH system is equal to the sum of the installed capacity of the distributed systems represented in the case study, and it is connected to node 7. The examination shows that the distributed PtH systems reduce the total amount of power imported from the main grid, as indicated in Fig. 10. For instance, for Alpha equal to 0.01, 0.1, and 1, the amount of imported energy reduces

Table 6
Sensitivity analysis of the MOGP approach.

Weighted coefficients	Z_1(\$)	Z_2(kWh)	Weighted coefficients	Z_1(\$)	Z_2(kWh)
$\omega_1 = 1$ and $\omega_2 = 0$	1272.95	18219.13	$\omega_1 = 0.4$ and $\omega_2 = 0.6$	1740.12	11649.59
$\omega_1 = 0.8$ and $\omega_2 = 0.2$	1314.47	14434.91	$\omega_1 = 0.2$ and $\omega_2 = 0.8$	2816.43	7027.54
$\omega_1 = 0.6$ and $\omega_2 = 0.4$	1359.71	13934.74	$\omega_1 = 0$ and $\omega_2 = 1$	6566.00	−115.08

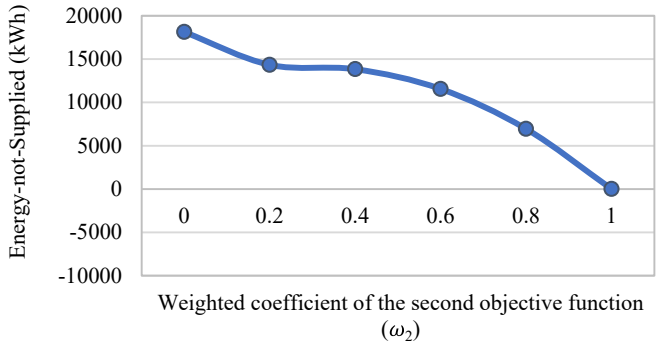

Fig. 14. Energy-not-supplied versus different weighted coefficients for resiliency consideration objective function.

by 610 kWh, 470 kWh, and 410 kWh, respectively. It shows a more efficient operation of the PtH systems to deal with changes in demand when installed in a distributed way compared to a centralized one. More precisely, in the distributed installation of the PtH systems, more output power of renewable energy resources is converted and charged into hydrogen storage systems. As a result, this can assist demand provision more efficiently and reduce the dependency on the main grid. On the other hand, when the price of hydrogen increases, the amount of imported energy rises as well, from 18.12 MWh to 26.92 MWh. However, the reason is that the hydrogen production to be sold to industries is more beneficial when there is a high price of hydrogen and compen-

Table 7
Examining different weighted coefficients for each term of the second objective function.

Weighted coefficient of $\mathscr{R}_1$	Weighted coefficient of $\mathscr{R}_2$	Weighted coefficient of $\mathscr{R}_3$	Z_2
0.2	0.4	0.4	9996.470
0.5	0.25	0.25	3481.525
0.8	0.1	0.1	2238.990
0.4	0.2	0.4	1858.448
0.25	0.5	0.25	1161.530
0.1	0.8	0.1	464.612
0.4	0.4	0.2	1791.199
0.25	0.25	0.5	1245.591
0.1	0.1	0.8	699.982

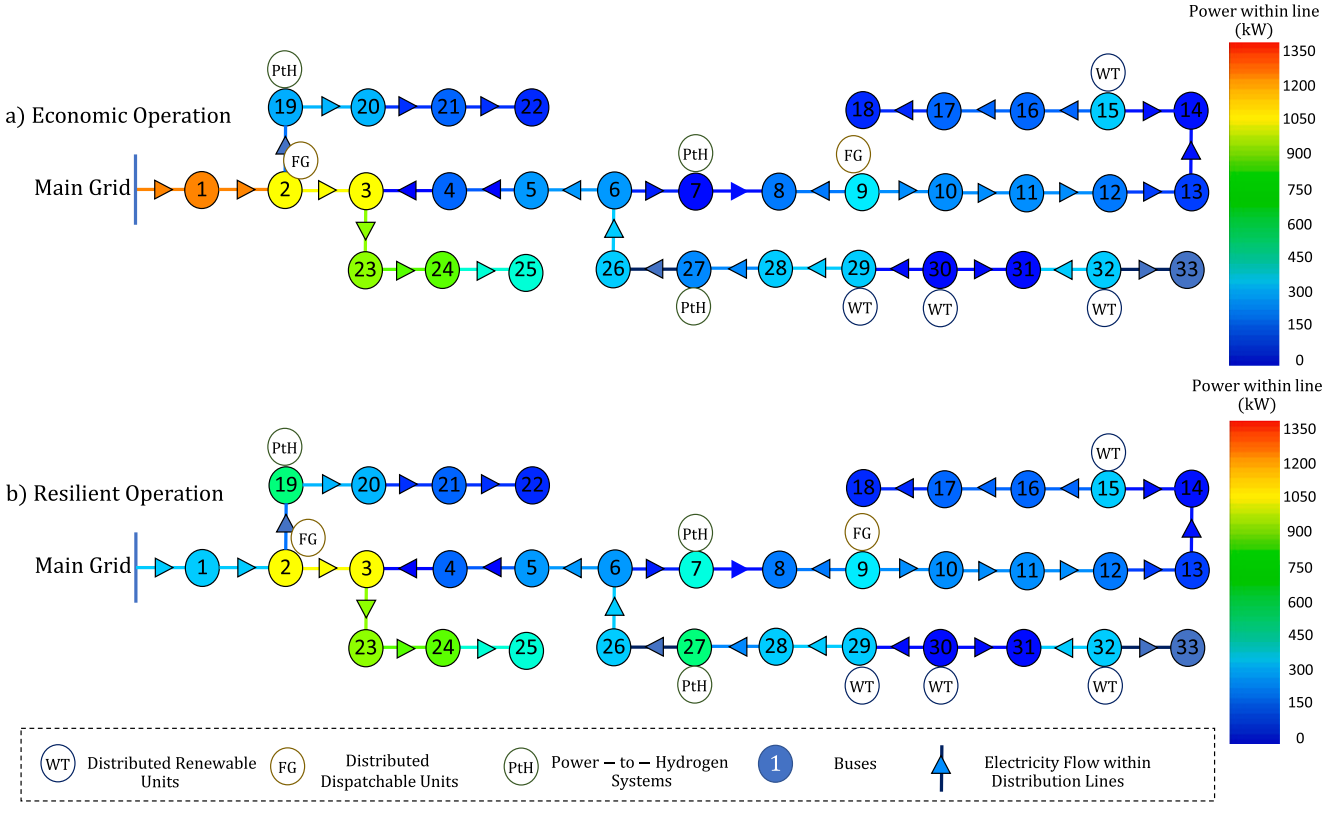

Fig. 15. Load flows through microgrid with and without resiliency consideration ((a) economic operation and (b) resilient operation).

Table 8
Comparison of costs and solving time using GAMS software versus GBD.

Weighted coefficients	Solver	Z_1($)	Solving Time (sec)
$\omega_1 = 1$ *and* $\omega_2 = 0$	DICOPT	1009.50	733
	GBD	1009.51	330
$\omega_1 = 0.8$ *and* $\omega_2 = 0.2$	DICOPT	1314.47	954
	GBD	1314.47	418
$\omega_1 = 0.6$ *and* $\omega_2 = 0.4$	DICOPT	1359.71	987
	GBD	1359.70	433
$\omega_1 = 0.4$ *and* $\omega_2 = 0.6$	DICOPT	1740.12	1263
	GBD	1740.12	558
$\omega_1 = 0.2$ *and* $\omega_2 = 0.8$	DICOPT	2816.43	1244
	GBD	2816.42	550
$\omega_1 = 0$ *and* $\omega_2 = 1$	DICOPT	6566.00	1800
	GBD	6566.00	810

sating operating costs. To go into greater depth, the operating cost of the microgrid and the amount of produced emission in this scenario is indicated in Fig. 11. In the figure, in addition to the centralized and distributed PtH systems, another case is examined without the PtH systems when Alpha is equal to 0.01. Based on the obtained results, the distributed integration of PtH systems, compared to when there are no PtH systems, reduces the emissions by two tons and the cost of operation by $540. It is due to the reduction in the amount of imported power from the main grid due to the more efficient operation of PtH systems to deal with the variable output of renewable resources and changes in demand. More precisely, the distributed PtH systems are more efficiently charged in off-peak hours and discharged during peak hours which assists demand provision in this case. However, it should be noted that the centralized PtH systems can normally provide a higher efficiency due to economies of scale, optimized operation, and large-scale production, which should not be ignored [73].

All in all, the analyses in this subsection can provide microgrid operators with proper insights into the operation of the PtH systems. Firstly, the analyses show that the integration of the PtH systems can supply either the demand of industries for hydrogen or electricity demand during peak hours. It depends on the strategy of the operators and the price of hydrogen whether the hydrogen must be sold to industries to increase the revenue (i.e., compensate the cost of operation) or consumed in the microgrid for other purposes, such as peak shaving that prevent the establishment of extra capacity of suppliers. Besides, the analyses prove that the installation of the system in a distributed way makes these systems operate more efficiently. It concludes with more cost-saving and emission reduction compared to a centralized high-capacity PtH system.

4.2. Resiliency analysis and computational performance of the decomposition approach

In this subsection, at first, analysis is conducted to examine the potential of PtH systems in the resilient operation of the microgrid. To this aim, the scheduling of the microgrid in the absence of PtH systems is indicated in Fig. 12 (i.e., Scenario 3). The hourly scheduling of the microgrid indicates that it is more dependent on the main grid (especially during the peak operating hours) instead of charging PtH systems during off-peak and valley hours of demand and discharging them during peak hours. In comparison with Fig. 6, it is evident that wind curtailment occurred from 00:00 to 07:00 and from 23:00 to 24:00. It means that although wind power is available, it cannot be used in the microgrid due to some limitations (e.g., congestion). However, as discussed earlier, the output power of turbines could be converted to hydrogen to be used during peak hours of the operating period. It should be noted that, in this case, the total wind curtailment during the operating period is 4.5 MWh.

The scheduling of the microgrid with and without PtH systems in a day with a low wind power availability is also indicated in Fig. 13 to investigate the value of PtH systems in extreme conditions (i.e., Scenario 4). It is assumed that, in the presence of PtH systems, at the beginning of the operating period, the hydrogen storage systems are full (e.g., due to the availability of wind power and/or low price of energy in previous days). It shows that when a low amount of wind power is available, the microgrid supplies a large portion of demand by purchasing from the main grid (especially when there are no PtH systems). However, the microgrid's dependency on hydrogen-to-power to supply demand is evident from 07:00 to 21:00. It indicates the positive role of PtH systems in the energy management of microgrids to enhance resilience.

In this subsection, the obtained results of the resiliency consideration approach are investigated. In Table 6, the sensitivity analysis of weighted coefficients of the MOGP approach is indicated. When the weighted coefficient of the first objective (i.e., Cost minimization (Z_1)) increases from zero to one, the cost of operation reduces from $6566.00 to $1272.95. However, the resiliency reduces due to some reasons, such as dependency on the main grid and low levels of hydrogen within the tanks. On the other hand, the increase in the weighted coefficient of the second objective function (i.e., de-resilience minimization (Z_2)) reduces the de-resilience from 18219.13 to −115.08. It is noteworthy to mention that the greater the weighted coefficient is given to the second objective (i.e., resiliency consideration), the more cost of operation increases. For instance, when ω_2 increases from 0 to 0.6, the operating cost goes up from $1272.95 to $1740.12. However, when the weighted coefficient is equal to 0.8 and 1, the operating cost is considerably elevated, matching $2816.43 and $6566.00, respectively. The reason is that a considerable amount of hydrogen within tanks is stored when the weighted coefficient of the second objective is high. It also highlights the role of the PtH systems in the economic operation of the microgrid. As the cost of operation surges when a considerable level of hydrogen is stored within the tanks, the most resilient approach would not be preferable from the economic perspective, although improving the resiliency of the microgrid.

In Fig. 14, the changes in the amount of energy-not-supplied versus the weighted coefficient of the resiliency consideration objective function are demonstrated in the case of the main grid failure. This analysis is conducted by fixing all decision variables based on the obtained result from the optimization problem (i.e., scheduling of microgrid) except the

Table 9
Data of demand, wind output power, and electricity price during a day.

Time (hour)	Electricity (%)	Wind (%)	Electricity price ($/kWh)	Time (hour)	Electricity (%)	Wind (%)	Electricity price ($/kWh)
1	0.6843	0.8345	0.0300	13	0.9460	0.7601	0.1600
2	0.6451	0.5361	0.0200	14	0.9515	0.5987	0.0850
3	0.6198	0.4424	0.0300	15	0.9721	0.4704	0.0820
4	0.6044	0.4220	0.0250	16	0.9991	0.5162	0.0700
5	0.6057	0.9124	0.0250	17	1.0000	0.5641	0.0800
6	0.6268	0.8579	0.0310	19	0.9638	0.6466	0.0650
7	0.6773	0.8981	0.0450	19	0.9608	0.8375	0.0550
8	0.7437	0.6792	0.0470	20	0.9271	0.9480	0.0650
9	0.8029	0.9266	0.0490	21	0.9269	0.8187	0.0750
10	0.8484	0.9083	0.0620	22	0.8872	0.9185	0.0500
11	0.8930	0.8075	0.0900	23	0.7853	0.9699	0.0450
12	0.9222	1.0000	0.1300	24	0.7685	0.9002	0.0350

load shedding and the objective function value. The amount of interactions with the main grid is also equal to zero in the case of this failure to simulate islanded mode of operation. As demonstrated in the figure, as far as the weighted coefficient of the second objective function increases from zero to one, the amount of energy-not-supplied reduces when there is an interruption in the main grid. Although having a considerable amount of cost (see the last table), when ω_2 is equal to one, there is no load shedding during the islanded mode, which is preferable from the resiliency viewpoint.

Additional analysis is conducted to investigate the underlying reasons for the no load shedding during resilient operation scenarios. This analysis aims to identify the factors and conditions that contribute to the successful avoidance of load shedding, providing insights into the effectiveness of the resilient operation strategy. In Fig. 15, the load flow within the microgrid is indicated for the most economic strategy of operation versus the most resilient one in the peak hour ($t = 17$). It is worthwhile mentioning that the microgrid is still connected to the main grid. The analysis shows that the amount of power imported from the main grid reduces in the resilient operation (b) in comparison with the economic operation (a). In this mode, the dispatchable generating units connected to node two operate to supply a considerable portion of demand. However, the cost of these generating units is more than the price of the main grid. Moreover, in the resilient operation, the maximum volume of hydrogen is stored within tanks connected to nodes 7, 19, and 27 to deal with the predicted failure of the main grid. As a result, when the microgrid goes to the islanded mode in the case of failure in the main grid, no load shedding occurs.

Another analysis is also conducted to examine the impact of each term of the second objective function on the resiliency (i.e., the impact of $\mathscr{R}_1$, $\mathscr{R}_2$, and $\mathscr{R}_3$ on Z_2). This analysis is conducted considering the most resilient approach, examined above ($\omega_1 = 0$ and $\omega_2 = 1$). For this purpose, determining a weighted coefficient for each term of the second objective function, the value of this objective function (de-resiliency) is examined as demonstrated in Table 7. Based on the analysis, when the weighted coefficient of the second term is higher than other ones (weighted coefficient of $\mathscr{R}_2$ is equal to 0.8), the maximum resiliency (i.e., minimum de-resiliency) is achieved. It highlights the impact of the availability of hydrogen to be converted to electricity in emergency cases (e.g., islanded model when local supply is lower than demand). Moreover, this term makes the objective function exclusive, as when the amount of hydrogen stored in storage systems increases, it concludes the increase in the operating cost of the microgrid. The reason is that the microgrid should purchase more power from the main grid and/or dispatch gas-fired units.

To sum up, it should be declared that it is beneficial to sell hydrogen to industries in a normal situation. However, when a failure in the main grid is predicted, and local supply is lower than demand, it is not reasonable. In the case of prediction of failure in the main grid, the hydrogen produced by PtH systems must be stored within tanks to be converted to electricity after the failure occurrence. It prevents or reduces energy-not-supplied in the microgrid in the case of the occurrence of the predicted event. Aside from the mentioned strategy, two other measures are employed in this research that prevent load shedding, including the reduction in interactions with the main grid and power loss. The former decreases the dependency on the main grid and the latter causes supply demand from the nearest producers. Therefore, whenever a microgrid goes to islanded mode, if the strategies are implemented beforehand, the amount of shedding reduces significantly, which prevents harming the industries. Industries are negatively affected by a shortage of electrical power, as material is lost, equipment breaks down, and productivity is lost.

Aside from the discussed issues, the cost of microgrid operation versus various levels of resilience is examined. For this purpose, both the GAMS DICOPT solver and the GBD method are integrated into the MOGP method to solve the optimization problem considering different weighted coefficients. It should be noted that this GAMS solver is mainly used to solve complex problems, whose benefits are generating high-quality solutions and faster computation. Table 8 compares the value of the objective function and the solving time between the GBD method and DICOPT to ensure that the proposed approach yields unique solutions. This comparison serves to evaluate the performance of both methods in terms of solution quality and computational efficiency. It is demonstrated that the integration of GBD provides better or similar solutions in a shorter time. When the economic aspect is only considered ($\omega_1 = 1$), the decomposition approach reduces the solving time from 733 s to 330 s. However, in the most resilient approach ($\omega_2 = 1$), the integration of the GBD to solve the problem decreases the solving time from 1800 s to 810 s. It should be noted that when$\omega_1 = 0.8$, 0.6, 0.4, and 0.2, the GBD reduces the solving time by 536, 554, 678, and 694 s, respectively. Besides, when the problem is solved using the GBD approach, upper and lower bounds converge between eight to ten iterations. For instance, in Fig. 16, the convergence to the optimal solution is depicted in eight iterations when $\omega_1 = 1$ and $\omega_2 = 0$ as well as $\omega_1 = 0$ and $\omega_2 = 1$.

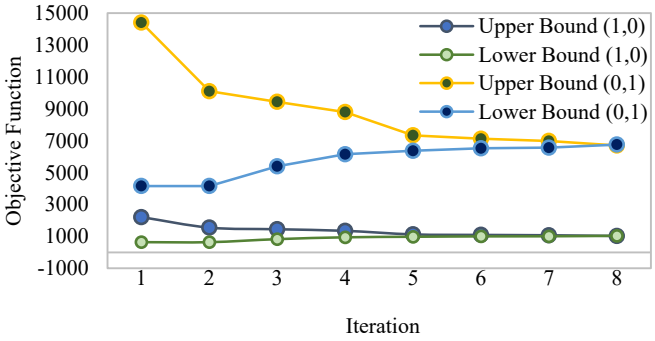

Fig. 16. Convergence of upper and lower bounds using the GBD.

5. Conclusion

This study introduced a bi-objective optimization model formulated as a mixed-integer nonlinear programming problem. The model was specifically designed for the resilient operation of microgrids that incorporate power-to-hydrogen systems which include electrolyzers, hydrogen storage systems, and fuel cells. The power-to-hydrogen systems produced hydrogen from excess electricity in the microgrid, which could either be sold to industry or stored in tanks for future use. Three resilience measures were considered in this study to improve microgrid operation during main grid failures: (i) decreasing imported power, (ii) reducing power loss, and (iii) increasing hydrogen levels in the tanks. The decrease in the amount of imported power from the main grid and power loss measures reduced the dependency of the microgrid on the main grid. As a result, the electricity was supplied from the nearest resources, improving the reliability of supply. The increase in hydrogen level in the tanks improved the ability of the microgrid to supply the demand in the islanded mode by utilizing the stored hydrogen for conversion to electricity. To address the complexity of the mixed-integer nonlinear programming bi-objective model for the operation of the industrial microgrid, a novel method was developed. This method integrated the Generalized Benders Decomposition technique with the Multi-Objective Goal Programming approach. The aim was to handle the model's complexity while improving computational performance effectively.

Based on the results, the integration of the power-to-hydrogen system into the microgrid could either facilitate the provision of peak electricity demand or supply the required amount of hydrogen in the industries. The price of hydrogen plays a crucial role in determining the most beneficial course of action: whether to sell hydrogen to industries (in the case of a high hydrogen price) or convert it into electricity (in the

case of a low hydrogen price). The price directly influences the economic viability and profitability of these options, allowing decision-makers to optimize their strategy based on prevailing market conditions. Furthermore, three cases of (i) no power-to-hydrogen system, (ii) a centralized power-to-hydrogen system, and (iii) distributed power-to-hydrogen systems were considered, and cost and emissions analyses were carried out. It was demonstrated that the distributed integration of power-to-hydrogen systems reduced the emissions by about 20 % and the operating cost by about 30 % compared to the no power-to-hydrogen system case, due to the reduction in the amount of power imported from the main grid. In the low wind power availability scenario, it was indicated that the power-to-hydrogen systems were important in maintaining the security of supply and enhancing system resilience. The study investigated the impact of different weighted coefficients on the role of resilience measures. Furthermore, the computational performance of the problem was evaluated with respect to the solution approach used. The approach of resilience consideration indicated that the most resilient weighted coefficients increased the operation cost by more than four times. However, in this case, the amount of load shedding in the case of failure of the main grid was zero. It was also demonstrated that the solution time of this mixed-integer nonlinear programming problem was reduced by 54 % using the developed approach compared to GAMS commercial solver.

While this study offers valuable insights into the resilient operation of microgrids with power-to-hydrogen systems, there are additional areas that warrant further exploration. One such aspect is the incorporation of costs associated with the establishment and maintenance of power-to-hydrogen system components, including electrolyzers, storage systems, and fuel cells. Future research can delve into integrating these cost considerations into the optimization model to provide a more comprehensive analysis of the economic feasibility and viability of such systems in ensuring a reliable and sustainable energy supply. Besides, future studies can focus more on incorporating uncertainty in the model. This can involve exploring the effects of different sources of uncertainty, such as availability of renewable power and electricity demand.

CRediT authorship contribution statement

Vahid Shahbazbegian: Data curation, Investigation, Methodology, Software, Writing – original draft. **Miadreza Shafie-khah:** Conceptualization, Supervision, Validation, Writing – review & editing. **Hannu Laaksonen:** Conceptualization, Supervision, Validation, Writing – review & editing. **Goran Strbac:** Supervision, Writing – review & editing. **Hossein Ameli:** Investigation, Methodology, Visualization, Writing – review & editing.

Declaration of Competing Interest

The authors declare that they have no known competing financial interests or personal relationships that could have appeared to influence the work reported in this paper.

Data availability

Data will be made available on request.

Acknowledgment

Hossein Ameli & Goran Strbac gratefully acknowledge the EPSRC-funded program “High efficiency reversible solid oxide cells for the integration of offshore renewable energy using hydrogen ”under grant number EP/W003597/1 as well as from European Union’s Horizon 2020 research and innovation program "GreenHyScale" under grant agreement No 101036935.

Appendix A. Electricity network data

The shares of electricity demand (hourly demand/peak demand) and wind output power (available power/installed capacity) as well as electricity price during the day are indicated in Table 9 [49].

In Table 10 and Table 11, the characteristics of the electricity network and the electricity demand are demonstrated, respectively. It is noteworthy to mention that the demand is indicated as active and reactive powers, and it is assumed all loads have the same profile [74].

Table 11
Microgrid’s load.

Node	Load (kW + jkVar)	Node	Load (kW + jkVar)
2	100 + j60	18	90 + j40
3	90 + j40	19	90 + j40
4	120 + j80	20	90 + j40
5	60 + j30	21	90 + j40
6	60 + j20	22	90 + j40
7	200 + j100	23	90 + j40
8	200 + j100	24	420 + j200
9	60 + j20	25	420 + j200
10	60 + j20	26	60 + j25
11	45 + j30	27	60 + j25
12	60 + j35	28	60 + j20
13	60 + j35	29	120 + j70
14	120 + j80	30	200 + j600
15	60 + j10	31	150 + j70
16	60 + j20	32	210 + j100
17	60 + j20	33	60 + j40

Table 10
Electricity network data.

Branch	From Node	To node	Resistance (Ω)	Reactance (Ω)	Branch	From Node	To node	Resistance (Ω)	Reactance (Ω)
1	1	2	0.0922	0.0470	17	17	18	0.7320	0.5740
2	2	3	0.4930	0.2511	18	2	19	0.1640	0.1565
3	3	4	0.3660	0.1864	19	19	20	1.5042	1.3554
4	4	5	0.3811	0.1941	20	20	21	0.4095	0.4784
5	5	6	0.8190	0.7070	21	21	22	0.7089	0.9373
6	6	7	0.1872	0.6188	22	3	23	0.4512	0.3083
7	7	8	0.7114	0.2351	23	23	24	0.8980	0.7091
8	8	9	1.0300	0.7400	24	24	25	0.8960	0.7011
9	9	10	1.0440	0.7400	25	6	26	0.2030	0.1034
10	10	11	0.1966	0.0650	26	26	27	0.2842	0.1447
11	11	12	0.3744	0.1238	27	27	28	1.0590	0.9337
12	12	13	1.4680	1.1550	28	28	29	0.8042	0.7006
13	13	14	0.5416	0.7129	29	29	30	0.5075	0.2585
14	14	15	0.5910	0.5260	30	30	31	0.9744	0.9630
15	15	16	0.7463	0.5450	31	31	32	0.3105	0.3619
16	16	17	1.2890	1.7210	32	32	33	0.3410	0.5302

References

[1] Galvin R. Are electric vehicles getting too big and heavy? Modelling future vehicle journeying demand on a decarbonized US electricity grid. Energy Policy 2022;161:112746. https://doi.org/10.1016/J.ENPOL.2021.112746.

[2] Blumberg G, Broll R, Weber C. The impact of electric vehicles on the future European electricity system – A scenario analysis. Energy Policy 2022;161:112751. https://doi.org/10.1016/J.ENPOL.2021.112751.

[3] Bowen T, Koebrich S, McCabe K, Sigrin B. The locational value of distributed energy resources: A parcel-level evaluation of solar and wind potential in New York state. Energy Policy 2022;166:112744. https://doi.org/10.1016/J.ENPOL.2021.112744.

[4] Debouza M, Al-Durra A, EL-Fouly THM, Zeineldin HH. Survey on microgrids with flexible boundaries: Strategies, applications, and future trends. Electr Pow Syst Res 2022;205:107765. https://doi.org/10.1016/J.EPSR.2021.107765.

[5] Khodaei A. Resiliency-oriented microgrid optimal scheduling. IEEE Trans Smart Grid 2014;5:1584–91. https://doi.org/10.1109/TSG.2014.2311465.

[6] Powering farming futures: Establishing a case for microgrids | Australian Cane Grower n.d. https://search.informit.org/doi/10.3316/informit.992112572803650 (accessed February 18, 2023).

[7] Satsangi KP, Das DB, Babu GSS, Saxena AK. Real time performance of solar photovoltaic microgrid in India focusing on self-consumption in institutional buildings. Energy Sustain Dev 2019;52:40–51. https://doi.org/10.1016/J.ESD.2019.07.001.

[8] Millstein D, Dobson P, Jeong S. The potential to improve the value of U.S. geothermal electricity generation through flexible operations. J Energy Resour Technol, Trans ASME 2021:143. https://doi.org/10.1115/1.4048981/1089719.

[9] Thema M, Bauer F, Sterner M. Power-to-Gas: Electrolysis and methanation status review. Renew Sustain Energy Rev 2019;112:775–87. https://doi.org/10.1016/J.RSER.2019.06.030.

[10] Farrokhifar M, Nie Y, Pozo D. Energy systems planning: A survey on models for integrated power and natural gas networks coordination. Appl Energy 2020;262:114567. https://doi.org/10.1016/J.APENERGY.2020.114567.

[11] Niu M, Wan C, Xu Z. A review on applications of heuristic optimization algorithms for optimal power flow in modern power systems. J Mod Power Syst Clean Energy 2014;2:289–97. https://doi.org/10.1007/S40565-014-0089-4/METRICS.

[12] Faisal S. A Review of Integrated Energy System with Power to Gas Technology. European Journal of Electrical Engineering and Computer. Science 2020:4. https://doi.org/10.24018/EJECE.2020.4.6.260.

[13] Aljabery AAM, Mehrjerdi H, Mahdavi S, Hemmati R. Multi carrier energy systems and energy hubs: Comprehensive review, survey and recommendations. Int J Hydrogen Energy 2021;46:23795–814. https://doi.org/10.1016/J.IJHYDENE.2021.04.178.

[14] Son YG, Oh BC, Acquah MA, Fan R, Kim DM, Kim SY. Multi Energy System with an Associated Energy Hub: A Review. IEEE Access 2021;9:127753–66. https://doi.org/10.1109/ACCESS.2021.3108142.

[15] Liu Z, Wang H, Zhou B, Yang D, Li G, Yang B, et al. Optimal Operation Strategy for Wind–Hydrogen–Water Power Grids Facing Offshore Wind Power Accommodation. Sustainability 2022, Vol 14, Page 6871 2022;14:6871. https://doi.org/10.3390/SU14116871.

[16] Li B, Li X, Su Q. A system and game strategy for the isolated island electric-gas deeply coupled energy network. Appl Energy 2022;306:118013. https://doi.org/10.1016/J.APENERGY.2021.118013.

[17] Ding X, Sun W, Harrison GP, Lv X, Weng Y. Multi-objective optimization for an integrated renewable, power-to-gas and solid oxide fuel cell/gas turbine hybrid system in microgrid. Energy 2020;213:118804. https://doi.org/10.1016/J.ENERGY.2020.118804.

[18] Chen H, Song J, Zhao J. Synergies between power and hydrogen carriers using fuel-cell hybrid electrical vehicle and power-to-gas storage as new coupling points. Energy Convers Manag 2021;246:114670. https://doi.org/10.1016/J.ENCONMAN.2021.114670.

[19] Guo Q, Nojavan S, Lei S, Liang X. Potential evaluation of power-to-hydrogen-to methane conversion technology in robust optimal energy management of a multi-energy industrial park. Int J Hydrogen Energy 2021;46:33039–52. https://doi.org/10.1016/J.IJHYDENE.2021.07.148.

[20] Yang Y, Tang L, Wang Y, Sun W. Integrated operation optimization for CCHP micro-grid connected with power-to-gas facility considering risk management and cost allocation. Int J Electr Power Energy Syst 2020;123:106319. https://doi.org/10.1016/J.IJEPES.2020.106319.

[21] Liu B. Optimal scheduling of combined cooling, heating, and power system-based microgrid coupled with carbon capture storage system. J Energy Storage 2023;61:106746. https://doi.org/10.1016/J.EST.2023.106746.

[22] Wang Y, Yang Y, Fei H, Song M, Jia M. Wasserstein and multivariate linear affine based distributionally robust optimization for CCHP-P2G scheduling considering multiple uncertainties. Appl Energy 2022;306:118034. https://doi.org/10.1016/J.APENERGY.2021.118034.

[23] Zhang Z, Altalbawy FMA, Al-Bahrani M, Riadi Y. Regret-based multi-objective optimization of carbon capture facility in CHP-based microgrid with carbon dioxide cycling. J Clean Prod 2023;384:135632. https://doi.org/10.1016/J.JCLEPRO.2022.135632.

[24] Mobasseri A, Tostado-Véliz M, Ghadimi AA, Reza Miveh M, Jurado F. Multi-energy microgrid optimal operation with integrated power to gas technology considering uncertainties. J Clean Prod 2022;333:130174. https://doi.org/10.1016/J.JCLEPRO.2021.130174.

[25] Lekvan AA, Habibifar R, Moradi M, Khoshjahan M, Nojavan S, Jermsittiparsert K. Robust optimization of renewable-based multi-energy micro-grid integrated with flexible energy conversion and storage devices. Sustain Cities Soc 2021;64:102532. https://doi.org/10.1016/J.SCS.2020.102532.

[26] Chen JJ, Qi BX, Rong ZK, Peng K, Zhao YL, Zhang XH. Multi-energy coordinated microgrid scheduling with integrated demand response for flexibility improvement. Energy 2021;217:119387. https://doi.org/10.1016/J.ENERGY.2020.119387.

[27] Li Y, Zhang F, Li Y, Wang Y. An improved two-stage robust optimization model for CCHP-P2G microgrid system considering multi-energy operation under wind power outputs uncertainties. Energy 2021;223:120048. https://doi.org/10.1016/J.ENERGY.2021.120048.

[28] Tabar VS, Jirdehi MA, Jordehi AR. A robust multi-objective joint scheduling of integrated electricity and gas grids considering high penetration of wind and solar units and flexible loads towards achieving a sustainable operation. Int J Hydrogen Energy 2023;48:4613–30. https://doi.org/10.1016/J.IJHYDENE.2022.11.028.

[29] Tostado-Véliz M, Arévalo P, Jurado F. A comprehensive electrical-gas-hydrogen Microgrid model for energy management applications. Energy Convers Manag 2021;228:113726. https://doi.org/10.1016/J.ENCONMAN.2020.113726.

[30] Salehi J, Namvar A, Gazijahani FS, Shafie-khah M, Catalão JPS. Effect of power-to-gas technology in energy hub optimal operation and gas network congestion reduction. Energy 2022;240:122835. https://doi.org/10.1016/J.ENERGY.2021.122835.

[31] Najafi A, Pourakbari-Kasmaei M, Jasinski M, Lehtonen M, Leonowicz Z. A max–min–max robust optimization model for multi-carrier energy systems integrated with power to gas storage system. J Energy Storage 2022;48:103933. https://doi.org/10.1016/J.EST.2021.103933.

[32] MansourLakouraj M, Niaz H, Liu JJ, Siano P, Anvari-Moghaddam A. Optimal risk-constrained stochastic scheduling of microgrids with hydrogen vehicles in real-time and day-ahead markets. J Clean Prod 2021;318:128452. https://doi.org/10.1016/J.JCLEPRO.2021.128452.

[33] Nourollahi R, Salyani P, Zare K, Mohammadi-Ivatloo B. Resiliency-oriented optimal scheduling of microgrids in the presence of demand response programs using a hybrid stochastic-robust optimization approach. Int J Electr Power Energy Syst 2021;128:106723. https://doi.org/10.1016/J.IJEPES.2020.106723.

[34] Masrur H, Sharifi A, Islam MR, Hossain MA, Senjyu T. Optimal and economic operation of microgrids to leverage resilience benefits during grid outages. Int J Electr Power Energy Syst 2021;132:107137. https://doi.org/10.1016/J.IJEPES.2021.107137.

[35] Vahedipour-Dahraie M, Rashidizadeh-Kermani H, Anvari-Moghaddam A. Risk-Based Stochastic Scheduling of Resilient Microgrids Considering Demand Response Programs. IEEE Syst J 2021;15:971–80. https://doi.org/10.1109/JSYST.2020.3026142.

[36] Liu J, Cao X, Xu Z, Guan X, Dong X, Wang C. Resilient operation of multi-energy industrial park based on integrated hydrogen-electricity-heat microgrids. Int J Hydrogen Energy 2021;46:28855–69. https://doi.org/10.1016/J.IJHYDENE.2020.11.229.

[37] Vahedipour-Dahraie M, Rashidizadeh-Kermani H, Anvari-Moghaddam A, Siano P, Catalão JPS. Short-term reliability and economic evaluation of resilient microgrids under incentive-based demand response programs. Int J Electr Power Energy Syst 2022;138:107918. https://doi.org/10.1016/J.IJEPES.2021.107918.

[38] Silva JAA, López JC, Arias NB, Rider MJ, da Silva LCP. An optimal stochastic energy management system for resilient microgrids. Appl Energy 2021;300:117435. https://doi.org/10.1016/J.APENERGY.2021.117435.

[39] Liu G, Ollisben T, Zhang Y, Jiang T, Tomsovic K. Robust Microgrid Scheduling with Resiliency Considerations. IEEE Access 2020;8:153169–82. https://doi.org/10.1109/ACCESS.2020.3018071.

[40] Jia L, Kandaperumal G, Pannala S, Srivastava A. Coordinating Energy Resources in an Islanded Microgrid for Economic and Resilient Operation. Conference Record - IAS Annual Meeting (IEEE Industry Applications Society) 2021;2021-October. https://doi.org/10.1109/IAS48185.2021.9677050.

[41] Ghiasi M, Niknam T, Dehghani M, Siano P, Alhelou HH, Al-Hinai A. Optimal Multi-Operation Energy Management in Smart Microgrids in the Presence of RESs Based on Multi-Objective Improved DE Algorithm: Cost-Emission Based Optimization. Applied Sciences 2021, Vol 11, Page 3661 2021;11:3661. https://doi.org/10.3390/APP11083661.

[42] Mandal S, Mandal KK. Optimal energy management of microgrids under environmental constraints using chaos enhanced differential evolution. Renew Energy Focus 2020;34:129–41. https://doi.org/10.1016/J.REF.2020.05.002.

[43] Phani Raghav L, Seshu Kumar R, Koteswara Raju D, Singh AR. Optimal Energy Management of Microgrids Using Quantum Teaching Learning Based Algorithm. IEEE Trans Smart Grid 2021;12:4834–42. https://doi.org/10.1109/TSG.2021.3092283.

[44] Roy NB, Das D. Optimal allocation of active and reactive power of dispatchable distributed generators in a droop controlled islanded microgrid considering renewable generation and load demand uncertainties. Sustain Energy Grids Networks 2021;27:100482. https://doi.org/10.1016/J.SEGAN.2021.100482.

[45] Gholami K, Dehnavi E. A modified particle swarm optimization algorithm for scheduling renewable generation in a micro-grid under load uncertainty. Appl Soft Comput 2019;78:496–514. https://doi.org/10.1016/J.ASOC.2019.02.042.

[46] Jiao PH, Chen JJ, Peng K, Zhao YL, Xin KF. Multi-objective mean-semi-entropy model for optimal standalone micro-grid planning with uncertain renewable energy resources. Energy 2020;191:116497. https://doi.org/10.1016/J.ENERGY.2019.116497.

[47] Dey B, Márquez FPG, Basak SK. Smart Energy Management of Residential Microgrid System by a Novel Hybrid MGWOSCACSA Algorithm. Energies 2020, Vol 13, Page 3500 2020;13:3500. https://doi.org/10.3390/EN13133500.

[48] Yang J, Su C. Robust optimization of microgrid based on renewable distributed power generation and load demand uncertainty. Energy 2021;223:120043. https://doi.org/10.1016/J.ENERGY.2021.120043.
[49] Luo L, Abdulkareem SS, Rezvani A, Miveh MR, Samad S, Aljojo N, et al. Optimal scheduling of a renewable based microgrid considering photovoltaic system and battery energy storage under uncertainty. J Energy Storage 2020;28:101306. https://doi.org/10.1016/J.EST.2020.101306.
[50] Li Q, Liao Y, Wu K, Zhang L, Lin J, Chen M, et al. Parallel and Distributed Optimization Method with Constraint Decomposition for Energy Management of Microgrids. IEEE Trans Smart Grid 2021;12:4627–40. https://doi.org/10.1109/TSG.2021.3097047.
[51] Khaligh V, Ghezelbash A, Mazidi M, Liu J, Ryu JH, Na J. A stochastic agent-based cooperative scheduling model of a multi-vector microgrid including electricity, hydrogen, and gas sectors. J Power Sources 2022;546:231989. https://doi.org/10.1016/J.JPOWSOUR.2022.231989.
[52] Mohammadi A, Mehrpooya M. A comprehensive review on coupling different types of electrolyzer to renewable energy sources. Energy 2018;158:632–55. https://doi.org/10.1016/J.ENERGY.2018.06.073.
[53] Yusaf T, Fernandes L, Talib ARA, Altarazi YSM, Alrefae W, Kadirgama K, et al. Sustainable Aviation—Hydrogen Is the Future. Sustainability 2022, Vol 14, Page 548 2022;14:548. https://doi.org/10.3390/SU14010548.
[54] Incer-Valverde J, Patiño-Arévalo LJ, Tsatsaronis G, Morosuk T. Hydrogen-driven Power-to-X: State of the art and multicriteria evaluation of a study case 2022. https://doi.org/10.1016/j.enconman.2022.115814.
[55] Shahbazbegian V, Ameli H, Shafie-Khah M, Laaksonen H, Ameli MT, Strbac G. Optimal Scheduling of Gas and Electricity Distribution Networks in Microgrids: A Decomposition Approach. In: 2022 IEEE International Conference on Environment and Electrical Engineering and 2022 IEEE Industrial and Commercial Power Systems Europe, EEEIC / I and CPS Europe; 2022 2022.. https://doi.org/10.1109/EEEIC/ICPSEUROPE54979.2022.9854624.
[56] Abbasi E, Ameli H, Strunz K, Duc NH. Optimized operation, planning, and frequency control of hybrid generation-storage systems in isolated networks. IEEE PES Innovative Smart Grid Technologies Conference Europe 2012. https://doi.org/10.1109/ISGTEUROPE.2012.6465719.
[57] Macedo LH, Franco JF, Romero R, Rider MJ. An MILP model for the analysis of operation of energy storage devices in distribution systems. 2016 IEEE PES Transmission and Distribution Conference and Exposition-Latin America, PES T and D-LA 2016 2017. https://doi.org/10.1109/TDC-LA.2016.7805610.
[58] Gu X, Hou Z, Cai J. Data-based flooding fault diagnosis of proton exchange membrane fuel cell systems using LSTM networks. Energy and AI 2021;4:100056. https://doi.org/10.1016/J.EGYAI.2021.100056.
[59] Zhao J, Jian Q, Huang Z, Luo L, Huang B. Experimental study on water management improvement of proton exchange membrane fuel cells with dead-ended anode by periodically supplying fuel from anode outlet. J Power Sources 2019;435:226775. https://doi.org/10.1016/J.JPOWSOUR.2019.226775.
[60] Hosseini-Motlagh SM, Samani MRG, Shahbazbegian V. Innovative strategy to design a mixed resilient-sustainable electricity supply chain network under uncertainty. Appl Energy 2020;280:115921. https://doi.org/10.1016/J.APENERGY.2020.115921.
[61] Geoffrion AM. Generalized Benders decomposition. J Optim Theory Appl 1972;10:237–60. https://doi.org/10.1007/BF00934810/METRICS.
[62] Karbowski A. Generalized Benders Decomposition Method to Solve Big Mixed-Integer Nonlinear Optimization Problems with Convex Objective and Constraints Functions. Energies 2021, Vol 14, Page 6503 2021;14:6503. https://doi.org/10.3390/EN14206503.
[63] Kundu T, Islam S. An interactive weighted fuzzy goal programming technique to solve multi-objective reliability optimization problem. J Ind Eng Int 2019;15:95–104. https://doi.org/10.1007/S40092-019-0321-Y/FIGURES/4.
[64] Farivar M, Low SH. Branch flow model: Relaxations and convexification-part i. IEEE Trans Power Syst 2013;28:2554–64. https://doi.org/10.1109/TPWRS.2013.2255317.
[65] Floudas C. Nonlinear and mixed-integer optimization: fundamentals and applications. 1995.
[66] Nonlinear and Mixed-Integer Optimization: Fundamentals and Applications - Christodoulos A. Floudas - Google Books n.d. https://books.google.fi/books?hl=en&lr=&id=OhTfOjSkq18C&oi=fnd&pg=PR11&dq=C.+A.+Floudas,+Nonlinear+and+Mixed-Integer+Optimization:+Fundamentals+and+Applications.+Oxford+University+Press,+USA,+1995.&ots=soruH6wRDy&sig=ORahlBPdcozUCv2YIAxQflcKb5o&redir_esc=y#v=onepage&q&f=false (accessed May 12, 2023).
[67] Scutari G, Facchinei F, Song P, Palomar DP, Pang JS. Decomposition by partial linearization: Parallel optimization of multi-agent systems. IEEE Trans Signal Process 2014;62:641–55. https://doi.org/10.1109/TSP.2013.2293126.
[68] Roshanaei V, Luong C, Aleman DM, Urbach DR. Reformulation, linearization, and decomposition techniques for balanced distributed operating room scheduling. Omega (Westport) 2020;93:102043. https://doi.org/10.1016/J.OMEGA.2019.03.001.
[69] Yue M, Lambert H, Pahon E, Roche R, Jemei S, Hissel D. Hydrogen energy systems: A critical review of technologies, applications, trends and challenges. Renew Sustain Energy Rev 2021;146:111180. https://doi.org/10.1016/J.RSER.2021.111180.
[70] Li Z, Zheng Z, Xu L, Lu X. A review of the applications of fuel cells in microgrids: opportunities and challenges. BMC Energy 2019 1:1 2019;1:1–23. https://doi.org/10.1186/S42500-019-0008-3.
[71] Albaker A, Majzoobi A, Zhao G, Zhang J, Khodaei A. Privacy-preserving optimal scheduling of integrated microgrids. Electr Pow Syst Res 2018;163:164–73. https://doi.org/10.1016/J.EPSR.2018.06.007.
[72] Rezvani A, Gandomkar M, Izadbakhsh M, Ahmadi A. Environmental/economic scheduling of a micro-grid with renewable energy resources. J Clean Prod 2015;87:216–26. https://doi.org/10.1016/J.JCLEPRO.2014.09.088.
[73] Ikäheimo J, Weiss R, Kiviluoma J, Pursiheimo E, Lindroos TJ. Impact of power-to-gas on the cost and design of the future low-carbon urban energy system. Appl Energy 2022;305:117713. https://doi.org/10.1016/J.APENERGY.2021.117713.
[74] Mahdavi M, Alhelou HH, Cuffe P. Test Distribution Systems: Network Parameters and Diagrams of Electrical Structural. IEEE Open Access J Power Energy 2021;8:409–20. https://doi.org/10.1109/OAJPE.2021.3119183.